PhD degree in Systems Medicine

(Curriculum in Human Genetics)

European School of Molecular Medicine (SEMM),

University of Milan and University of Naples "Federico II"

Molecular Biology

Unraveling a new role of TFEB in filopodia formation

Serena Raimo

TIGEM, Pozzuoli

Mat. R10756 - R20

Supervisor: Prof. Andrea Ballabio

TIGEM, Pozzuoli

Added Supervisor: Prof. Carmine Settembre

TIGEM, Pozzuoli

Academic Year 2017-2018

501-Mel	501-Melanocyte
ARP2/3	Actin-Related Protein 2/3
BCL2	B-Cell Lymphoma 2
bHLH-Zip	Basic Helix-Loop-Helix leucine-Zipper
BIRC7	Baculoviral IAP Repeat-Containing protein 7
Ca^{2+}	Calcium
CDC42	Cell Division Control Protein42
CLEAR	Coordinator Lysosomal Expression And Regulation
Dia2	Diaphanous-related Formin-2
ECM	Extra Cell Matrix
EPS8	Epidermial growth factor receptor Pathway Substrate 8
ERK2	Extracellular signal-Regulated Kinase 2
GTPase Rheb	GTPase Ras Homolog enriched in Brain
hbss	Hank's Balanced Salt Solution
IRSp53	Insulin-Receptor Substrate p53
MCOLN1	Mucolipin 1
MENA	Mammalian-Enabled
MiT familily	Microphthalmia-associated Transcription family
MITF	MIcrophthalmia-associated Transcription Factors
MT1-MMP	membrane type 1 metalloprotease
mTORC1	Mechanistic Target Of Rapamycin Complex 1
MYOX	Myosin X
N-WASP	Neuronal Wiskott-Aldrich syndrome protein
NEU1	Neuraminidase1
PDAs	Pancreatic Ductal Adenocarcinomas
PtdIns(4,5)P2	phosphatidylinositol-4,5-bisphosphate
RAC1	RAC family small GTPase 1
Rag	RAs-related GTP-binding

RCC	Renal Cell Carcinoma
RhoA	Ras Homolog family member A
RIF	Rho In Filopodia
TFE3	Transcription Factor E3
TFEB	Transcription Factor EB
TFEC	Transcription Factor EC
v-ATPase	Vacuolar-type H+ ATPase
w/o aa	With out amino acids
WASP	Wiskott-Aldrich Syndrome protein
WAVE2	WASP-family verprolin-homologous 2

Abstract

Chapter 1

Introduction

Chapter 2

Aims of the Thesis

Unraveling a new role of TFEB in controlling cell invasion by regulating actin cytoskeleton remodeling

Chapter 3

Materials and Methods

Chapter 4

Results

4.1 TFEB overexpression in different cell lines causes a drastical change in cell shape

4.2 Bioinformatics analysis reveals the presence of CLEAR binding sites in promoters of actin and filopodia related genes

4.3 TFEB activation causes an increase in mRNA level of filopodia genes in HeLa cell

4.4 TFEB depletion causes a decrease in mRNA level of EPS8 and IRSp53 genes in HeLa cell

4.5 TFEB overexpression causes an increase in protein level of EPS8 and IRSp53 in HeLa cell

Abstract

The microphthalmia family (MITF, TFEB, TFE3, and TFEC) of transcription factors is emerging as global regulators of cancer cell survival and energy metabolism, both through the promotion of lysosomal genes as well as newly uncharacterized targets. During my Ph.D. thesis project, I revealed a new set of TFEB target genes that when activated could contribute to cell migration and invasiveness in cancer. During my work, I found that TFEB regulates the filopodial initiator's factors IRSp53 and EPS8 causing a change in cell shape and an increase in filopodia number that correlates with an augmented motility and invasiveness of the cell. On the contrary, depletion of TFEB and TFE3 leads to down-regulation of EPS8 and IRSp53, and a decrease of filopodia numbers. I confirmed the entire study in the Melanoma cell line (501Mel), a model of cancer, that are cells with a high degree of motility, showing that also in this system, there is an increase in the number of filopodia as well as of EPS8 and IRSp53 levels. This phenotype was completely reversed by depletion of MITF or TFEB and TFE3, demonstrating that the upregulation of these transcription factors could contribute to the invasive phenotype of melanoma cells.

Altogether these data revealed a new role of MITF transcription factors as regulators of a transcriptional program that could control metastatic cancer initialization.

Chapter1

Introduction

1.1 MiT/TFE family of bHLH-LZ transcription factors

The transcription factor EB (TFEB) is a member of microphthalmia family of basic helix-loop-helix leucine-zipper (bHLH-Zip) transcription factors (MiT family).

MiT family is composed of 4 different factors: microphthalmia-associated transcription factor (MITF), TFEB, TFE3 and TFEC[1] (Fig. 1).

All the factors of MiT family share a common basic region needed to DNA binding sequence and involved in their dimerization; outside of this identical region, they differ in all the others regions[1], and while TFEB, TFE3 and MITF are more similar among themselves sharing the same activation domain[2, 3] ; this domain lacks in TFEC, that it appears to be more divergent factor and seems to be involved in a negative feedback loop mechanism working as inhibitor rather than activator [4].

All the members of the MiTs family are able to bind a palindromic sequence CACGTG E-box; this motif is also recognized by other bHLH-Zip transcription factors as MYC or MAX or MAD[5], although MiT transcription factors are the only one that can bind a non palindromic, asymmetric sequence TCATGTG M-box[6]. Moreover, MiT transcription members are able to form of both homodimers and heterodimers with any members of the family [5,7], but they are not able to form

heterodimers with other members of bHLH-Zip transcription factors family[5].

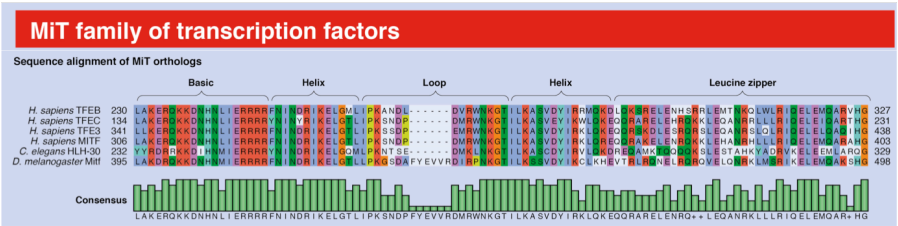

Fig. 1 MiT family of transcription factors. (Image adapted from Napolitano et al., 2016)

Furthermore, the protein members of the MiT family are all conserved in vertebrates; a single MiT component is ortholog and is found in invertebrate organisms; indeed, in Drosophila melanogaster the only component present is called *Mitf* [8], whereas, in Caenorhabditis elegans there is *HLH-30*[9]. The orthologs MiT present in invertebrates conserve the basic regions and HLH-Zip domains[10], suggesting that they are able to bind DNA in a way that is similar to mammalian MiT members.

The presence of a single transcription factor in invertebrates suggests that a common ancestral gene underwent multiple rounds of duplication, and this allowed a functional specialization of 4 different mammalian MiT proteins[10].

1.1.1 Transcription factor EB (TFEB) as master regulator of lysosomal function

Lysosomes are specialized organelles, containing an array of enzymes that are important for degradation of waste materials inside of the cell.

Because of their prominent role in intracellular degradation, lysosome has been viewed as a “static” organelle that performs “routine” work for the cell, mostly pertaining degradation and recycling of cellular waste. In recent years, however, this perception of lysosomes, as more degradative organelles, has started to change with the realization that they participate in many other cellular processes like secretion, plasma membrane repair, signaling, energy metabolism, tumor invasion and metastasis (Fig. 2)[11]. Moreover, lysosome-based signaling and degradation are subject to reciprocal regulation, indeed transcriptional programs control the biogenesis, the composition, and the abundance of lysosomes and fine-tune their activity to match the metabolic needs of the cell[12,13].

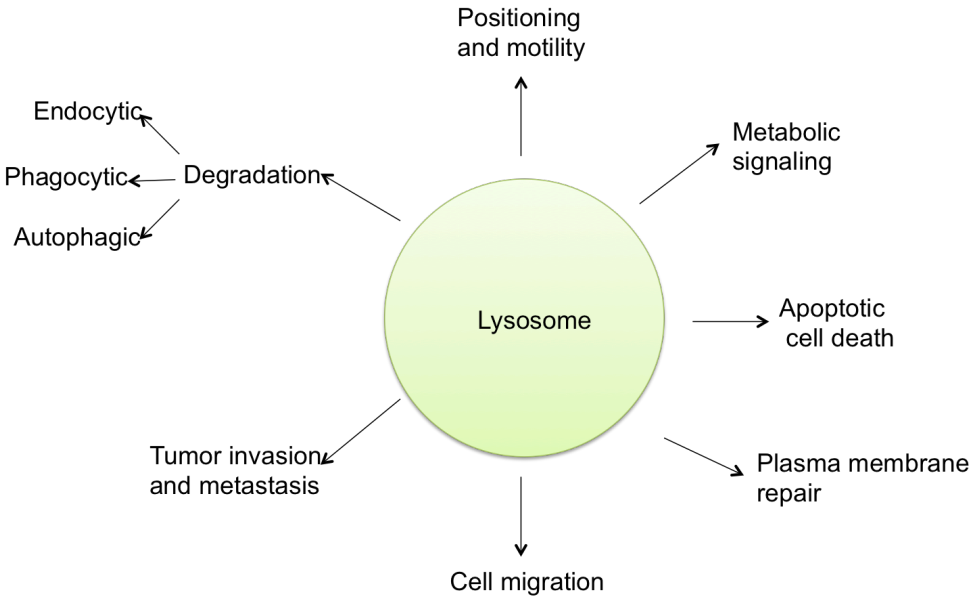

Fig. 2 Different cellular process in which are involved lysosomes (Image adapted from Jing et al., 2016)

A recent and important discovery shows that TFEB, a member of MiT family, is the master transcription factor that controls this transcriptional program[14].

Bioinformatic analysis of lysosomal promoter genes showed the presence of a common 10-bases E-box-like palindromic sequence called Coordinated Lysosomal Expression And Regulation "CLEAR" motif. This sequence is recognized and directly bound by TFEB, promoting the expression of the entire gene network, that share the CLEAR sequence[15, 16].

Indeed, when TFEB is overexpressed, there is an increase in lysosome number and in the production of lysosomal enzymes; the increase of lysosomes number and lysosomal enzymes lead to clearance of the storage materials by promoting the ability of

cells to degrade lysosomal substrates[15], resulting in an enhancement of catabolic pathway.

Moreover, it has been demonstrated that TFEB is involved in the regulation of many others pathways that involve lysosomal functions like autophagy and lysosomal exocytosis[16] (Fig. 3).

Indeed, the CLEAR site is present in the promoter of several "autophagy-related" genes by which TFEB activation can promote the biosynthesis of new autophagosomes, but also the fusion between lysosomes and autophagosomes[17].

TFEB is also able to induce the clearance of undigested materials by a process called lysosomal exocytosis[18] by which lysosomes can fuse with the plasma membrane and secrete the digested material outside the cell.

Definitely, TFEB can be considered the master regulator of the transcriptional programs that controls the logic of the cellular metabolic organization by regulating lysosomal activity. Indeed, alterations of this interconnection cause the pathophysiology of an ever-expanding spectrum of conditions, including storage disorders, neurodegenerative diseases, and cancer.

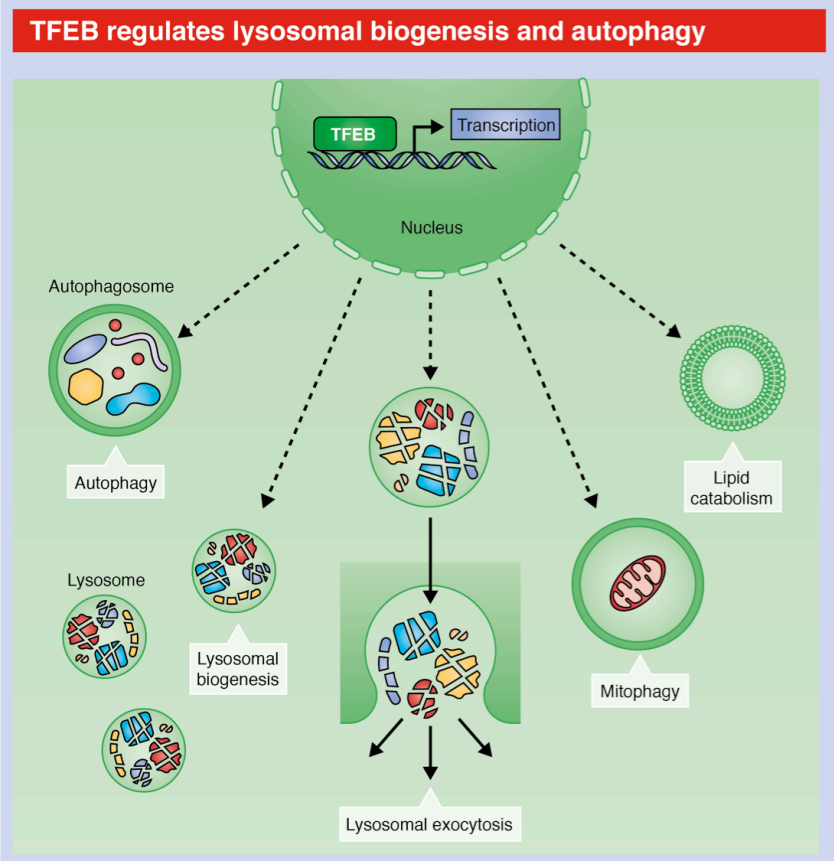

Fig. 3 TFEB regulated processes (Image adapted from Napolitano et al., 2016) TFEB positively regulates the transcription of several genes involved in lysosomal biogenesis, lysosomal proliferation, lysosomal exocytosis and induce the expression of the genes involved in autophagic pathways, in mitophagy pathways and in lipid catabolisms.

1.1.2 TFEB regulation

Since TFEB is a master regulator of cellular catabolism, its activity is highly regulated by post transduction modification, protein interaction and localization inside the cell[19] (Fig. 4).
TFEB localization and activity depends on different and multiple phosphorylation states. There are two different serines that play

a crucial role in TFEB activation. When TFEB is phosphorylated on S142[17,20] and S211[20,21,22] it is blocked into the cytoplasm in its inactive status[15,17]. When TFEB is dephosphorylated, it is able to translocate to the nucleus where it is able to activate its target genes. Nutrient deprivation, starvation or lysosomal stress are the conditions by which TFEB translocate to the nucleus. Mutation Ser-to-Ala, for both S142 and S211, results in a TFEB constitutively and active, that stays into the nucleus[21,22,17,20].

In rich nutrient conditions, two kinases, mechanistic target of rapamycin complex 1 (mTORC1), and extracellular signal-regulated kinase 2 (ERK2) [21,22,17,20] regulate TFEB phosphorylation.

In this condition, mTORC is recruited on lysosomes membrane[23] by the small Ras-related GTP-binding (Rag); Rag is previously activated by the v-ATPase complex present on lysosomes, that in turn is activated by GTPase Rheb[23-25].

Rag GTPase have a key role in TFEB phosphorylation because they are able to bind TFEB and block it on the lysosomal surface, promoting its phosphorylation by mTORC1[26].

In starvation condition, or in lysosomal stress condition, mTORC1 is released from the lysosome membrane and its inactive[23], at this point, TFEB is dephosphorylated by the phosphatase calcineurin; in turn, calcineurin is activated by the increase of Ca^{2+}, released from the lysosome through the Ca^{2+} channel mucolipin1 (MCOLN1)[27]; all these events promote TFEB nuclear translocation and its activation and upregulation; indeed,

in this condition TFEB is in active status and is able to activate itself in a positive feedback loop[28].

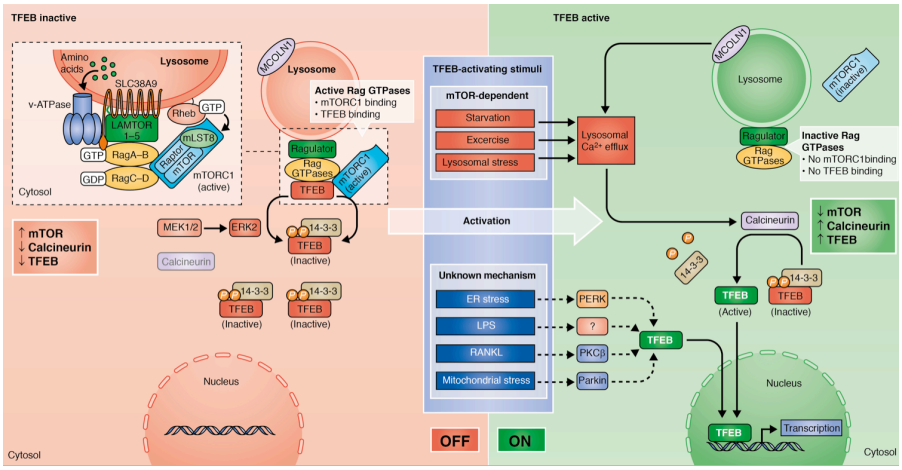

Fig. 4 TFEB regulation model (Image adapted from Napolitano et al., 2016) TFEB is induced by starvation and mediates the starvation response. In the presence of nutrients, TFEB interacts with the LYNUS machinery and is phosphorylated by mTORC1, on the lysosomal surface. This phosphorylation inactivates TFEB keeping it in the cytoplasm. During starvation, mTORC1 is no longer on the lysosome, and consequently, TFEB is not phosphorylated and it translocates into the nucleus, where it induces its own transcription and the transcription of its target genes, like the genes involved in the lysosomal-autophagy pathway.

The same regulation of TFEB occurs also for the other members of MiT family.

In nutrient availability TFE3 is sequestered on lysosomes by the binding with Rag GTPase, where it is phosphorylated by active mTORC1, resulting inactive[29].

Again, a similar activation mechanism is shared by MITF. It is phosphorylated by mTORC1 and, in this inactive state is retained on the lysosome by Rag GTPase[26].

1.2 TFEB and MiT family in tumorigenesis

In the past few years, mutations involving *TFEB*, *TFE3* and *MITF* genes had been identified in different cancerous condition. Amplifications and activating mutations of the MITF gene had been observed in melanoma, and in some forms of hereditary Renal Cell Carcinoma[30, 31], whereas chromosomal translocations leading to the overactivation of *TFEB* and *TFE3* genes had been identified in sporadic Renal Cell Carcinomas herein referred as *TFE*-fusion RCC[32].

It has been found that a switch of 6p21 to 11q13 results in a fusion of TFEB coding region with the regulator of non-coding *MALAT1* gene[33,34]. This event of translocation leads to a strong increase of TFEB full-length protein expression [35]. Altered TFEB expression or activity is associated with pancreatic cancer cell proliferation[36].

TFE3 translocation and fusion with different genes[37,38,39,40] are also associated with renal cell carcinoma (RCC): for example, the fusion between TFE3-ASPL leads to in alveolar soft part sarcoma[39].

Mutations in a single nucleotide of MITF gene[41], or amplification of MITF, are associated with an increase of 20% of solid tumor formation[42, 43] .

In general, constitutive activation of MiT family members is associated with pancreatic tumorigenesis and is fundamental for the growth of pancreatic ductal adenocarcinomas (PDAs)[44].

MiTF members can start the tumorigenesis process in a different way; they can directly upregulate cell cycle mediators, such as cyclin D2, D3 and p21[45,46]; moreover, they can induce the activation of anti-apoptotic genes, such as BCL2 or BIRC7 genes[47,48].

The overexpression of MiT members induces the upregulation of endo-lysosomal pathway that, in turn, can upregulate different tumorigenic signaling pathway, such as WNT pathway, that is altered in many types of cancer, and is the main actor of the initiation and progression of malignant modification[36,49,50].

Moreover, it has been demonstrated that kidney-specific TFEB overexpression in kidney mice, resulted in Renal Carcinoma and hepatic metastases. In these conditions, the samples revealed transcriptional induction and enhanced WNT b-catenin pathway. At the opposite hands, inhibitions of WNT signaling result in a significant rescue of the phenotype in vivo[51].

Finally, it has been demonstrated that mTORC1 lysosomal recruitment and activity depend directly by MiT/TFE transcription factors and that this feedback loop mechanism plays a role in cell hyperproliferation and cancer growth[52].

1.3 Filopodia molecular architecture and cellular role

The ability of cells to migrate in vivo is necessary for many physiological processes including embryonic development, tissue homeostasis and wound healing. Cell migration is also implicated in distinct pathological conditions such as inflammation and cancer metastasis[38].

Cell migration is one of the more studied processes; it depends on two different cellular protrusions, lamellipodia and filopodia.

Lamellipodia are very sheet-like thin protrusions, 0.1-0.2 μm filled with a branched network of actin.

Actin filament protrusions are polar structures. They could have different growth rates, myosin can bind actin filament in a phenomenon known as barbed end; or in contrast, the slowly growing is known as the pointed end.

For both filopodia and lamellipodia, the barbed end is oriented towards the plasma membrane, pushing against the leading edge and promoting the formation of protrusions and cellular migration or extension[53,54].

In the filopodium, some actin-bundling protein, as Fascin, are able to pack tightly the actin filament in parallel bundles against the plasma membrane.

This unidirectional organization allows for molecular motors, such MYOX, to transport several proteins along the filaments, to the filopodium tip. All these processes are useful to maintain the stability of the filopodia, but also to test the environment and cue

sensing, to establish the cell-cell junctions and for the transport of molecules to long-distances.

Historically, filopodia are considered as cellular “antennae” that are able to probe the environment; currently, it is known that filopodia play several and fundamental roles in physiologic processes.

Filopodia are involved in many different processes, including wound healing, adhesion to extracellular matrix, chemoattraction and embryonic development[55,56].

Cells can organize a transport of different molecules through filopodia, including receptors, from the inside of the cell to the tips. This phenomenon is crucial in many physiological processes including early embryonic development[57], tissue patterning[58,59], dendritic spine formation and mounting of an effective immune response[60].

One of the most studied functions of filopodia is the role that they play in cell migration; filopodia, indeed, are directly connected to cell migration thanks to their key functions that can improve cell motility. For this reasons, the abundance of filopodia at the edge leading to the cells is considered a characteristic of invasiveness in cancer cell[61].

Filopodia are able to transport, adhesion receptors, as well as cytokines from the base adhesion to the tips of filopodia allowing the cells to efficiently sense the environment. This type of transport is important to strengthen cell-cell junctions[62,63] and could be also involved in collective cell migration[64].

One more role of filopodia in cell migration is linked to ECM tethering and probing through the transport of cell-ECM adhesion receptors to filopodia tips. Indeed, transporting integrins, a family of adhesion receptors, filopodia play a central role also in modulating cell adhesion; it is therefore not a surprise that many cells use filopodia in early phases of spreading[65-67].

1.3.1 Filopodia formation

Small GTPases of Rho superfamily is the main actor involved in the regulation of cell morphology and, in particular, in the actin cytoskeleton.

The best known GTPases are Rac1, CDC42 and RhoA[68]; these three proteins have different roles in the regulation of actin cytoskeleton; Rac1 promotes lamellipodia formation, CDC42 is involved in filopodia formation and RhoA is implicated in stress fiber and focal adhesions[69].

There are different pathways that connect the action of CDC42 to the filopodia formation.

The most studied involves the activation of the complex ARP2/3, through activation of the two Nuclear Promoting Factors: WASP and N-WASP[70,71].

The interaction of CDC42 with WASP and N-WASP, together with phosphatidylinositol-4,5-bisphosphate (PtdIns(4,5)P_2), allow the

change of the auto inhibited conformation of WASP and subsequently activation of ARP2/3 complex[72].

A second and alternative mechanism of filopodia formation involves the insulin-receptor substrate p53 (IRSp53), which is an I-BAR-domain/IM-domain-containing protein. This is a quite large scaffold protein that is able to bind the small GTPase CDC42, its effector WAVE2 and the ENA/VASP family protein MENA, and in this big complex acts to increase the rate of the process of filopodia formation[73]. In literature, it is reported that IRSp53 bind MENA under the control of CDC42 to induce filopodia formation (Fig. 5A); but IRSp53 can also activate WAVE2, downstream Rac1, activates the actin filament nucleation of ARP2/3, and this complex, altogether, is able to induce lamellipodia formation[74,75] (Fig. 5B).

IRSp53 can specifically bind another protein, that is called EPS8[76]. IRSp53 and EPS8, are both weak bundlers; when they interact forming IRSp53: EPS8 complex their bundling action is synergistically enhanced. Together, they are able to bind the side of the actin filament and form a "filopodia initiation complex"[77] (Fig. 5).

Moreover, IRSp53 in addition to its role to recruit the actin regulator proteins to the site in which filopodia start, to assembler, induces membrane deformation, facilitating filopodia formation[78,79].

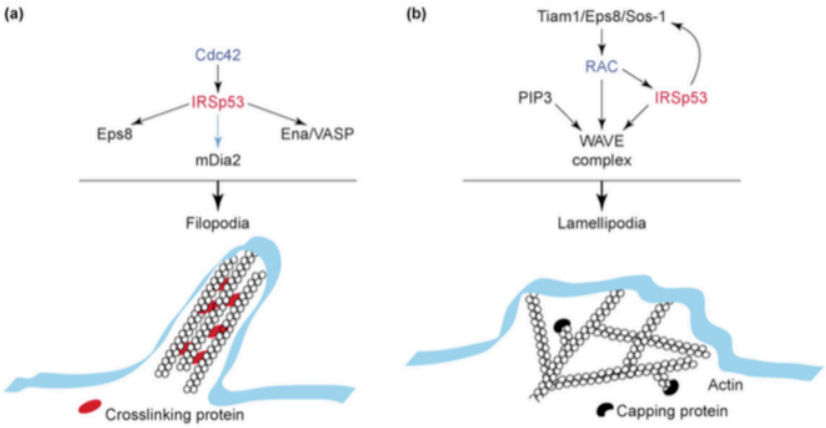

Fig. 5 Irsp53-based signaling circuitry regulating filopodia and lamellipodia extension (Adapted from Scita et al., 2008)

(a) Proposed model of the mechanism link Cdc42 to the IRSp53-based actin regulatory complex leading to the formation of filopodia; IRSp53 can be associated with activated Cdc42, and physically connecting this GTPase to Eps8 (an actin capper and bundling protein). The complex, localized to the plasma membrane, contribute to the generation and proper architectural organization of the linear actin bundles interconnected giving rise to filopodia

(b) Role of IRSp53 in mediating, through WAVE-based machinery, the extension of lamellipodia; The WAVE-based complex is key for the generation of the Arp2/3-dependent actin meshwork. IRSp53, thought to bind with WAVE complex, contributes to enhancing and confining its actin polymerization activity along the tip of extending protrusion, thus generating the forces required for lamellipodia

1.3.2 Molecular composition of filopodia

A large number of proteins are important to generate filopodia in different tissues and organisms.

ENA/VASP protein family is a relatively large group of proteins that, when is present Profilin protein, have anti-capping activity;

it means that they protect filaments from capping proteins[80-82]. ENA/VASP protein typically localize at focal adhesions, at cell-cell contacts, at the leading edge and/or at the tips of filopodia[83,84].

Formins are proteins that induce filopodia formation. They can form unbranched actin filaments by processed barber-end nucleation and elongation.

Myosins form a large family of motor proteins that are able to walk on actin filament to the filopodia tips. The unconventional MYOX induces filopodia formation, extension and stabilization [85].

Finally, Fascin, is an actin filament-bundling proteins, essential for the maintains of tight F-actin bundles of filopodia[86] (TAB. 1).

Table 1 | **Key proteins involved in filopodia formation**

Protein	Proposed activities and functions
CDC42	Small GTPase that induces filopodia formation
RIF	Small GTPase that promotes the formation of long filopodia through the formin protein Dia2
ARP2/3 complex	Actin filament nucleator that generates the formation of a branched lamellipodial F-actin network
WASP/ WAVE	Proteins that activate the F-actin nucleation activity of the ARP2/3 downstream of Rho family GTPases
Dia2	Protein that induces the formation of unbranched actin filaments in filopodia
ENA/VASP	Factors that promote actin filament elongation, anti-branching and/or bundling to induce filopodia formation
Myosin-X	Motor protein that promotes filopodia formation by converging filament barbed ends together and by transporting proteins to filopodial tips
Fascin	Major F-actin-crosslinking protein of filopodia
IRSp53	Scaffolding protein that also deforms membranes to promote the formation of plasma-membrane protrusions
LPR1	Lipid phosphatase-related protein that induces filopodia formation through a currently unidentified mechanism

TAB. 1 Adapted from Mattila et al., 2008

Historically, there were two different models of filopodia formation.

The first one is named “convergent elongation model”; this model predicts the filopodia formation from the lamellipodial F-actin network and a continue actin bundle extension of filopodia. According to this model, a subset of ARP2/3 complex-nucleated actin filaments is protected from capping and clustered with tip-complex proteins such as ENA/VASP, MYOX end Dia2[55].

The second model considers a “de novo” formation of filopodia; According to this model, they are nucleated at filopodial tips by formins.

To date, the working models show filopodia initiation by the convergence of uncapping and formin-nucleated actin filament. The elongation of the initial protrusion involves the use of mechanical forces to deform the plasma membrane. This process is enhanced by I-BAR domain protein, such as IRSp53. The subsequent elongation is allowed thanks to the crosslink with ENA/VASP and fascin; MYOX, in this model, is important to stabilize elongation phase, in addition to its role in the transportation of filopodial component to the tips[87] (Fig. 6).

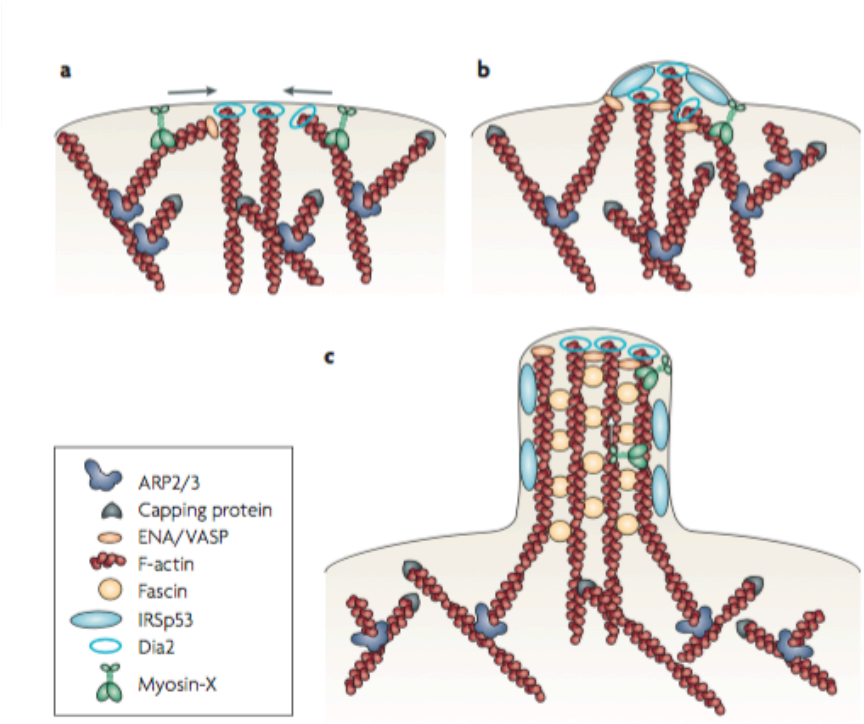

Fig. 6 A working model for filopodia formation (Adapted from Mattila et al.,2008)

The model describes the role of the different key proteins during filopodia formation.

a. A subset of existing uncapped actin filaments are targeted at the plasma membrane to be elongated by the Dia2 and by ENA/ VASP proteins. Moreover, Dia2 also nucleates the formation of new, unbranched actin filaments. The barbed ends of these elongating actin filaments are converged together through myosin-X, leading to the initiation of a filopodium.
b. When the preliminary filopodium begins to push the plasma membrane, IRSp53 facilitates plasma membrane protrusion deforming the plasma membrane.
c. The incorporation of fascin in the shaft of the filopodium generates a stiff actin filament bundle. At this stage, myosin-X localize in filopodium tip

1.3.3 Membrane protrusions at the leading edge

In order to move, the cell extends different types of protrusions from the plasma membrane, forward the leading edge[88].

The cells are able to extend lamellipodia, blebs and invadopodia to coordinate cell migration.

Lamellipodia come out from the thin sheet-like at the leading edge[89]. The dynamic lamellipodia protrude outside from the cells[88], from a more stable region, called lamella[90].

Invadopodia were first described as actin-rich matrix-degrading protrusion[91] because they are able to degrade the extracellular matrix during the invasion[92,93]. Invading cells extend their long protrusios three dimensions[93-95], to this end, the invadopodia use the force of actin polymerization.

The very difference between filopodia, lamellipodia and invadopodia is the degrade action, that is specific to invadopodia; Indeed, invadopodia contain vesicles with matrix-degrading proteases, in particular, membrane type 1 metalloprotease (MT1-MMP).

Finally, cells can migrate also thanks to blebs. They have been observed in multiple cancer cell[96,97].

The blebs formation depend on strong pressure against the plasma membrane[98]. In migrating cells, blebs are not retractable but new blebs are generated from existing one[99].

Filopodia, lamellipodia and blebs can coexist at the cellular leading edge; they are not exclusive[100]; although the presence of

filopodia and lamellipodia leads to a decrease of blebs and vice versa[101] because the mechanical processes of formation are opposite. Blebs require a decrease of actin filament interaction with the plasma membrane, on the other side, the formation of filopodia and lamellipodia require an increase of actin interaction with the plasma membrane.

1.3.4 Filopodia function in cancer cell invasion

Known the role of filopodia in cell migration, it is not surprising that filopodia have been associated and observed in the cancer cell and that they could have a role in migration and invasiveness in the tumor microenvironment[102]. Moreover, filopodia appear to be critical also in driving cancer cell metastasis and in the dissemination of carcinoma cell at secondary organs[103].

Clinical data suggest that filopodia have a fundamental role in cancer cell dissemination and many filopodial proteins are upregulated in human cancer cells.

The best example is Fascin; Fascin in completely absent in healthy epitelium[104] but is overexpressed in many metastatic cancers. Overexpression leads to an increase in motility and invasion[61,105] whereas, when Fascin is deleted the cell invasiveness is reduced[106].

Also, the regulation of MYOX is involved in different stages from healthy to cancer cell. Indeed, the expression of MYOX increases

in breast cancer[65,107], and the overexpression increases the number of filopodia per cells[108]. On the contrary, the silencing of MYOX inhibits the cellular invasion[65,107]. Moreover, it is known that MYOX is increased in the condition of p53 gain-of-function, a common feature of metastatic human cancer[65].

Other filopodia proteins are also implicated in cancer cell invasion, such as IRSp53 and EPS8, that are fundamental to initiate filopodia formation[67,109], the formin mDia2[110,111], and the cytoskeleton regulator ENA/VASP[112].

Chapter2

Aims of the Thesis

Historically, the transcription factor TFEB has been always considerate the master regulator of lysosome functions.

Indeed, as previously described in this thesis, it has been demonstrated that TFEB overexpression promotes all the steps of the lysosomes-autophagosomes axis, increasing the number of lysosomes and autophagosomes, the frequency of their fusion and the rate of substrate degradation[17]. These results indicated that TFEB is the true master regulator of cellular catabolism and coordinate the ability of the cell to respond and to adapt to external cues.

The goal of this project is to demonstrate a new and unknown role of TFEB as the master regulator of genes that are involved in actin remodelling. By preliminary experiments, I could observe that TFEB overexpression causes changes in cellular shape and increases in their ability to migrate. Starting of this preliminary data, the aim of my Ph.D. project has been the identification of the genes involved in the actin cytoskeleton remodeling and the formal demonstration of their direct regulation by TFEB.

In particular, I found that TFEB can regulate genes involved in the formation of filopodia and I revealed a molecular mechanism through which filopodia induction can mediate cancer cell invasiveness.

The specific aims of my Ph.D. project have been:

i) Validation of filopodia gene network in TFE transcription factors dependent way.

Starting from the observation that TFEB overexpression induces cell shape change and increase their ability to migrate, first, I generated a list of "actin-related" genes that could be the putative target of TFEB.

To validate these genes, I performed qRT PCR analysis in different experimental conditions and I identified EPS8 and IRSp53, two genes that play an important role in filopodia formation, as genes that are regulated by TFEB and TFE3. By using HeLa cells I found an increased level of RNA and protein of IRSp53 and EPS8 in TFE transcription factors overexpression and overactivation conditions, and, as expected, a decreased level of RNA and protein of these genes in TFE transcription factors KD conditions.

In agreement with these results, the number of filopodia was increased and decreased in the same experimental conditions, respectively.

By ChiP experiments, I also demonstrated that the EPS8 is a direct target of TFEB.

ii) Validation of the filopodia network in a Melanoma cell line

Using a model of the cancer cell, the melanoma cell line, 501-Mel, that shows high expression level of the MITF, I found an increased level of IRSp53 and EPS8 protein, and an increased number of the filopodia; phenotypes that were rescued by Knock-down of the MITF, TFEB, and TFE3 transcription factors.

Chapter3
Materials and Methods

3.1 Cell culture, treatments, transfections and plasmids

HeLa cell lines were purchased from ATCC and cultured in MEM (Invitrogen); The 501Mel cells were a kind gift from Ruth Halaban (26), and the A375P were from Colin Goding (27). 501Mel cells were cultured in RPMI (Invitrogen); All the cell lines were supplemented with 10% FBS, 1% penicillin/streptomycin and 2mM L-Glutamine (Euroclone). Cells were grown at 5% CO_2 at 37° C.

Starvation treatments were performed in HBSS-10mM Hepes or in RPMI media without amino acids supplemented with 10% FBS. Cells were rinsed twice with starvation medium, then kept in a full volume of starvation medium for 6h.

Human full-length TFEB-GFP, human full-length TFEB S142/211A, and human full-length TFE3-GFP were used in this study.

Cells were transfected with TransIT-LT1 Reagent (Mirus) following the manufacturer's protocol. All data are collected 48h post-transfection for RNA and protein analysis.

siRNAs were bought at Dharmacon. siRNA transfection was performed with Lipofectamine RNAi max (Invitrogen) using a reverse transfection protocols and plated in 6-well dishes. Cells transfected with siRNAs (20nM) were collected after 72h since transfection.

3.2 RNA isolation and reverse transcription

To obtain purified, high-quality (DNA-free) total RNA, RNA isolation from cell lines was used RNeasy Mini Kit (QIAGEN).
Before use, the β-Mercaptoethanol was added to Buffer RLT (RTL: β -Me = 100: 1). The cell pellets from confluent 100mm plates were suspended in Buffer RLT (700 μL). The volumes were added in QIAshredder columns and centrifuged at maximum speed for 3 minutes to fully homogenize the cells. The lysate is homogenized as it passes through the spin column. Then 1 volume of 70% ethanol was added to the eluate of each tube and mixed well by pipet. Ethanol is necessary to create conditions that promote selective binding of RNA to the RNeasy membrane. Thereafter, each sample has been transferred in RNeasy mini columns and the columns have been centrifuged at 10000 rpm for 30 seconds. The flow-through has been discarded. Then 700 μL of Buffer RW1 was added to each column and centrifuged at 11000 rpm for 30 seconds. Also, in this case, the flow-through has been discarded.
After 44 mL of 100% Ethanol was added to Buffer RPE and 500 μL of the final buffer was added to the columns, centrifuged at 11000 rpm for 30 seconds. The flow-through was discarded. This step has been repeated twice.
The RNeasy columns were transferred into fresh microcentrifuge tubes. RNase free water (30 μL) was added directly to the

columns and centrifuged at 11000 rpm for 1 minute. This step has been repeated by using the precedent eluate in order to obtain a higher final RNA concentration.

The final RNA concentration was determined by spectrophotometric analyses (Nanodrop technology), measuring the absorbance at 260 nm and the RNA purity was evaluated according to the A_{260}/A_{280} and A_{260}/A_{230} ratio.

RNA was converted into a complementary molecule of DNA (cDNA) through the reverse transcriptase enzyme and nonspecific primers (random primers) by using the QuantiTect Reverse Transcription Kit (QIAGEN). In particular, 1 μg RNA was reverse transcribed for each sample.

Purified RNA was incubated in gDNA Wipeout Buffer (2 μL) for 5 minutes at 42°C, to effectively remove contaminating genomic DNA.

Thereafter, 6 μL of master mix were added for each sample:

- 4 μL Quantiscript RT Buffer
- 1 μL Quantiscript Reverse Transcriptase
- 1 μL RT Primer Mix

They were incubated for 30 minutes at 42°C and for 3 minutes at 95°C.

Finally, they are diluted to obtain 33 ng/μL and stored at -20°C until used for qRT-PCR.

3.3 Real-Time PCR

qReal-Time PCR is a major development of PCR technology that enables reliable detection and measurement of products generated during each cycle of PCR process.

The process uses reverse transcription polymerase chain reaction (RT-PCR), coupled with fluorescent chemistry, to measure variations in transcriptome levels between samples. The amount of product is directly related to the fluorescence of a reporter dye.

qReal Time-PCR was performed by using Power SYBR Green PCR Master Mix (Roche).

SYBR Green I is an asymmetrical cyanine dye used as a nucleic acid stain in molecular biology. SYBR Green I bind to DNA. The resulting DNA-dye-complex absorbs blue light (λ_{max} = 497 nm) and emits green light (λ_{max} = 520 nm). Thus, an increase in DNA product during PCR, therefore, leads to an increase in fluorescence intensity measured at each cycle.

Every single reaction has a final volume of 20 µL which consists of:

- 7,5 µL of SYBR Green
- 1 µL of 10 µM forward primer and 1 µL of 10 µM reverse primer
- 2,5 µL of H_2O
- 3 µL of cDNA previously diluted with 130 ul of water

The mix for each gene analyzed and for GAPDH (Glyceraldehyde-3-phosphate dehydrogenase), which has been used to normalize mRNA levels, was prepared.
Each sample was analysed in duplicate and for each gene was used a negative control (mix where cDNA was replaced by the water). The experiment has been plated in a 96-well Real-Time PCR plate (LightCycler® 480 multiwell plate) and closed with a sealing foil giving protection against evaporation. The Real-Time plate was analysed by LightCycler® 96 Instrument (Roche).

The $2^{-\Delta\Delta Ct}$ formula was used to calculate the relative expression of the target gene.
The Ct (threshold cycle) value is the cycle number at which the fluorescence generated within a reaction crosses the fluorescence threshold, a fluorescent signal significantly above the background fluorescence. At the threshold cycle, a detectable amount of amplicon product has been generated during the early exponential phase of the reaction. The threshold cycle is inversely proportional to the original relative expression level of the gene of interest.

In details, it has been calculated:
- Average of each sample and its duplicate (MEDIA Ct);
- ΔCt: MEDIA Ct sample - MEDIA Ct of loading control;
- ΔΔCt: ΔCt treated samples - ΔCt untreated sample;
- Relative quantization: RQ= $2^{-\Delta\Delta Ct}$ for each ΔCt obtained.

The primers used in this study were reported in the table below.

PRIMERS	Forword	Reverse
CDC42	5'-TCTTCTCGGTTCTGGAGGCTC	5'-ACTGTCAAGTATATGTGGAGTGT
RIF	5'-GGAAGGAGCTGAAGATCGTG	5'-GTACTTCTCGAACACCGATGG
ARPc2	5'-GTGGTCATTGGAAAGGTGTTC	5'-GGTTCCCTGTGGCTAAAGAG
ARPc3	5'-GTGGTAGATTGAAGCCAAAACC	5'-GGCATACTTGGTAGAACTCAGG
WASP	5'-CCTACTTCATCCGCCTTTACG	5'-GTCATCTCCAGCGAAGGTG
WAVE	5'-AAATACCTTTGCCTCTCGGG	5'-GGTGTTGATTCCTTGCAGTG
mDIA2	5'-TTTCGTTATGTGCTCAATTGCCTT	5'-GTAAGGAAATGACTGGTGACCCC
FASCIN1	5'-AAAGTGTGCCTTCCGTACC	5'-CCACTCGATGTCAAAGTAGCAG
IRSp53	5'-GAGTTCTTTGGAGCCCTGG	5'-AGAATTACGAGAAGGCACTGG
EPS8	5'-CAGGTGGATGTTAGAAGTCGAG	5'-TTCCTGCTCATGATACTGCC
TFEB	5'-CCAGAAGCGAGAGCTCACAGAT	5'-TGTGATTGTCTTTCTTCTGCCG
TFE3	5'-GATGAGATCATCAGCCTGGA	5'-CAAGCAGATTCCCTGACACA
MITF	5'-GCTGGACAGGAGTTGCTGAT	5'-GGGCTTGATGGATCCTGCTT
RAGD	5'-AGGTGACAAAGTTCCTGGCT	5'-GCCGATTCTGAACCTTTCGA
MUCOLIPIN1	5'-TGGGACCCCAGCTTATTTATTT	5'-CTGTGTCCGATTCGATCAGC
NEU1	5'- CAGCACATCGAGTTCCGAG	5'-TGTCTCTTTCCGCCATGAGGT
HPRT	5'-GCCGATTCTGAACCTTTCGA	5'-GGTCCTTTTCACCAGCAAGCT

3.4 Protein extraction

To prepare samples for running on the polyacrylamide gel, cells need to be lysed to release proteins of interest.

Cell media was removed from the plates and the cells were washed twice with 1X PBS. PBS was removed as much as possible because excess liquid can decrease the concentration of lysates.

RIPA lysis buffer (50 mM Tris-HCl pH 7.5, 1% Triton X-100, 150 mM NaCl, 1 mM EDTA, 0.1% Na deoxicholate) was prepared by

adding protease inhibitor cocktail (1:100) and phosphatase inhibitors (1:1000).

It was added to the cell plates inappropriate amount and incubated for 10 minutes in order to be sure that RIPA is well distributed. Cells were scraped vigorously from the plate by using a plastic cell scraper that helps with the lysis process. Each cell lysate has been transferred in eppendorf and sonicated at appropriate intervals. Finally, the lysates were stored at -80°C until use.

3.5 BCA analysis

Protein extracts have been quantified by using the BCA protein assay.

The Pierce BCA Protein Assay is a detergent-compatible formulation based on bicinchoninic acid (BCA) for the colourimetric detection and quantitation of total protein. This assay primarily relies on two reactions.

First, the peptide bonds in proteins reduce Cu^{2+} ions to Cu^{+} (a temperature dependent reaction). The amount of Cu^{2+} reduced is proportional to the amount of proteins present in the solution. Next, two molecules of bicinchoninic acid chelate with each Cu^{+} ion, forming a purple-coloured product that strongly absorbs light at a wavelength of 562 nm.

The working solution has been prepared by mixing 50 parts of BCA Reagent A (containing sodium carbonate, sodium bicarbonate, bicinchoninic acid and sodium tartrate in 0.1 M sodium hydroxide) with 1 part of BCA Reagent B (containing 4% cupric sulphate).

Protein concentrations have been determined and reported with reference to standards of bovine serum albumin (BSA). A series of dilutions of known BSA concentration were prepared (0 µg/µl; 0,06 µg/µl; 0,125 µg/µl; 0,25 µg/µl; 0,5 µg/µl; 1 µg/µl and 2 µg/µl) and assayed alongside the unknowns samples. The protein concentration of each unknown sample has been determined based on the standard curve.

3.6 Western Blot Analysis

After the quantification of the proteins, it has been prepared 30 µg of proteins for each sample. It has been added 6X Laemmli buffer (4% SDS, 20% glycerol, 10% 2-mercaptoethanol, 0.004% bromphenol blue, 0.125 M Tris HCl) to samples.

The beta 2-mercaptoethanol reduces intra and inter-molecular disulfide bonds of the proteins. The SDS detergent binds to all the proteins positive charges which occur at a regular interval, thus giving each protein the same overall negative charge so that proteins will separate based on size and not by charge. The SDS also denatures the proteins to also help separate them based on

size, not on shape. Bromophenol blue serves as a migration indicator dye where it is possible to observe the dye front that runs ahead of the proteins. Bromophenol blue also functions to make it easier to see the sample during loading of the gel wells with protein sample. Glycerol in the Laemmli buffer increases the density of the sample so that it will fall to the bottom of the well, minimizing puffing or loss of protein sample in the buffer.

The protein samples were boiled for 5 minutes at 95° C and then loaded in 10% precast polyacrylamide gel to perform the SDS-PAGE (SDS-polyacrylamide gel electrophoresis) at 80V.

Before the end of running, PVDF membranes (*Millipore Immobilon™ PVDF Transfer Membranes) were activated with prior to use.* They were wet for 30 seconds in methanol. Then the membranes were transferred to purified water for at least 2 minutes. Finally, PVDF membranes were transferred in the transfer buffer (100 mL Blotting Buffer, 200 mL Methanol, 700 mL H_2O) and incubated for 5 minutes.

At the end of the running, the gel has been removed from its cast and gel and PVDF membranes were sandwiched between sponge and paper (sponge, paper, paper, gel, filter, paper, paper, sponge), making sure to get rid of air bubbles. It is important that the membrane is closest to the positive electrode and the gel closest to the negative electrode. Electroblotting has been performed for 1 hour at 4°C at 100 V.

This method is useful to further analyse proteins by using probes such as specific antibodies. Membranes were blocked in blocking buffer (5% skim milk in TTBS) for 1 hour at room temperature.

Primary antibodies have been diluted in blocking buffer and the membranes were incubated with the correct primary antibodies overnight at 4°C.

The day after the blots has been rinsed three times for 5 minutes at room temperature.

The filters have been incubated in horseradish peroxidase (HRP)- conjugated secondary antibody, diluted in blocking buffer, for 1 hour at room temperature. After 1 hour blots have been rinsed three times for 5 minutes at room temperature.

ECL (Enhanced ChemiLuminescence) has been used to detect the *antigen-antibody complexes on the blots.* The ECL solution contains a chemiluminescent substrate (luminol) and a strong oxidizing agent (hydrogen peroxide) that are then applied to the blot.

Horseradish peroxidise, in presence of hydrogen peroxide, catalyses the oxidation of luminol to 3-aminophthalate. The reaction is accompanied by the emission of low-intensity light at 428 nm. However, in the presence of certain chemicals, the light emitted is enhanced up to 1000-fold, making the light easier to detect and increasing the sensitivity of the reaction. The signal has been detected by Chemidoc instrument.

The primary and the correlative secondary antibody used in this project are in the table below.

AbI	diluition	AbII	**diluition**
EPS8 (BD)	1:1000	Anti-Mouse/HRP	1:10000
IRSp53 (SIGMA)	1:1000	Anti-Rabbit/HRP	1:10000
TFEB (Cell Signaling)	1:1000	Anti-Rabbit/HRP	1:10000
ACTIN (SIGMA)	1:3000	Anti-Mouse/HRP	1:10000

It has been used the software *ImageJ* to analyze western blot images. The quantification will reflect the amounts as a ratio of each protein band relative to the loading control band of the same lane.

3.7 Immunofluorescence Analysis

Immunofluorescence (IF) is a technique that uses the specificity of antibodies to their antigen to target fluorescent dyes (also called fluorophores or fluorochromes) to specific biomolecular targets. Antibodies that are chemically conjugated to fluorophores are commonly used. The fluorophore allows visualization of the target distribution in the sample under a fluorescent microscope (e.g. epifluorescence and confocal microscopes).

IF utilizes a two-step technique. In the first step, a primary unlabelled antibody binds to the target. In the second step, a secondary antibody (directed against the Fc portion of the

primary antibody), conjugated to a fluorophore, is used to detect the first antibody.

Cells have been grown, counted and plated directly on the coverslip.

The cell culture medium has been removed from the plates and the cells have been washed three times in PBS 1X. Then, cells have been fixed with 4% paraformaldehyde (PFA) for 10 minutes at room temperature. Fixation is needed to immobilize the antigens, while retaining authentic cellular and subcellular architecture. In particular, paraformaldehyde is a cross-linking reagent that forms intermolecular bridges, thus creating a network of linked antigens.

Fixed cells were washed three times with PBS 1X.

In order to permeabilize the cells and block unspecific binding of the antibodies, fixed cells have been covered with the Blocking Buffer for 30 minutes at room temperature.

Blocking Buffer has been prepared in PBS 1X and it is composed by:

- 3% BSA (Bovine Serum Albumin)
- 0,05 % Saponin

The specific primary antibodies, diluted in blocking buffer, over day at room temperature or overnight at 4°C, depending on the antibody.

The cells have been washed three times with blocking buffer for 5 minutes each.

Subsequently, cells have been incubated with secondary antibodies, diluted in blocking solution for 1 hour at room temperature in dark conditions. In particular, the secondary antibodies are raised against the host species used to generate the primary antibody.

After 1 hour of incubation, cells were washed three times with blocking solution for 5 minutes each.

Then, it has been added the DAPI (4',6-diamidino-2-phenylindole), diluted 1:1000 in blocking buffer, which is a fluorescent stain that binds strongly to A-T rich regions in DNA. When bound to double-stranded DNA, DAPI has an absorption maximum at a wavelength of 358 nm and its emission maximum is at 461 nm. It is useful to mark the nuclei.

After 15 minutes, cells were washed with PBS and coverslips have been mounted with a drop of mounting medium (ProLong® Gold Antifade Mountant).

The coverslips have been sealed with nail polish to prevent drying and movement under microscope and stored at 4°C.

Finally, the cells were imaged on a Carl Zeiss LSM 880 confocal microscope super resolution with a 63x oil immersion objective.

The primary and the correlative secondary antibody used in this project are in the table below.

AbI	diluition	AbII	diluition

TFEB (Cell Signaling)	1:400	Anti-Rabbit	1:800
TFE3 (SIGMA)	1:400	Anti-Rabbit	1:800
MYOX (SIGMA)	1:200	Anti-Rabbit	1:800
Phalloidin (Invitrogen)	1:200		1:800

The software *ImageJ* has been used to analyser files, to merge the different channels and to count the filopodia tips.

3.8 Cromatin immunoprecipitation analysis (ChIP)

For ChIP experiments were used a pure stable clone of HeLa cells that overexpress TFEB-3xFLAG; they were starved with HBSS, 10μM Hepes for 3 hours and then counted and analysed. The started sample contains $1x10^6$ cell.

The ChIP is a technic that allows to identifying specific DNA region that is bind by the protein of interest. It is based on the interaction of the ammine group present inside the proteins and the DNA basis, through the formaldehyde.

Cells were homogenised and fixed by formaldehyde 1% for 10 minutes at room temperature and then quenching using glycine 1x added at the resuspended cells.

At this point is important to isolate the DNA and for this reason, the cells are lysed; it is important to remove before the cytoplasm and then proceed to the lysis of the nucleus. Cells were washed three times in cold PBS 1X and then lysed in cell

lysis buffer (Pipes 5 mM pH 8.0, Igepal 0,5%, KCl 85 mM) for 15 min. Nuclei were lysed in nucleus lysis buffer (Tris HCl pH8.0 50mM, EDTA 10 mM, SDS 0.8 %) for 30 min.

DNA isolated it was fragmented using Covaris s220, in fragments of 200-500 bp by sonication with alternated cycles of 30''ON and 30''OFF for 15 times, and at this point, we obtain the immunocomplex that interacts with the protein of interest.

The sheared chromatin was immunoprecipitated overnight with anti-Flag SIGMA (6ug per sample) to recognise TFEB-3xFLAG present in overexpression in the stable clones used for ChIP experiments.

The immunoprecipitated chromatin was incubated 3 hours with magnetic protein G beads (Dynabeads Protein G, Invitrogen). Then, beads were washed with wash buffers and DNA eluted in elution buffer (Tris HCl pH8 50 mM, EDTA 1 mM, SDS 1%).

DNA was purified by ChIP DNA Clean and Concentrator kit (ZYMO RESEARCH) and it was analysed by RT-PCR. The primers used in this study are reported in the table below.

PRIMERS	**Forword**	**Reverse**
IRSp53	5'-CTTTCGTCTCCGTCCTGCTG	5'-GCATCTCCTCTGAGCGAGAC
EPS8	5'-CCCCATGCTGTCCTAACTTC	5'-CACAAAGCAAGCAAGTCCAA
MUCOLIPIN1	5'-GCCCGCCGCTGTCACTG	5'-AGGGGCTCTGGGCTACC
RLP30	5'-GGGGAACGAGAAAGGAAAGA	5'-CCTTCTGCTTGCGATCTGTT

In this study, the enrichment of the specific site of obtained is reported as %Input that means the quantity of DNA

immunoprecipitated normalized on the quantity of DNA present in the cells before the immunoprecipitation.

3.9 Cell Invasion Assay

For Cell Invasion Assay experiments were used a pure stable clone of HeLa cells that overexpress TFEB-3xFLAG and as control HeLa wt cells.

To start, the Invasion Chamber was adjusted at room temperature in a tissue culture hood and then was added 300µl of warm serum-free media to the interior of the inserts, to allow rehydrating the ECM layer for 1-2 hours at room temperature.

After that the membrane was rehydrated $0.5x10^6$ cells/ml was plated in serum-free media and complete media, containing 10% fetal bovine serum, was added to the lower chamber.

The experiment was left in the incubator for 30h.

Using a cotton-tipped swab gently was removed non-invading cells as well as the ECMatrix gel from the interior of the inserts. To be sure to remove cells on the inside perimeter, as any remaining cells inside the insert, the procedure with a clean cotton-tipped swab was repeated twice.

At this point, 500µl of staining solution was added to the unoccupied wells of the plate.

Stain invasive cells on the lower surface of the membrane by dipping inserts remain in the staining solution for 20 minutes.

Then the insert was washed in a beaker of water several times to rinse, and then the insert was left to air dry.

The images of the cells were taken by APOTOME ZEISS microscope, and the colourized invasive cells were counted by ImageJ tool “Count Cell”.

3.10 Wound Healing Assay

For Wound Healing assay was used a pure stable clone of HeLa cells that overexpress TFEB-3xFLAG and as control HeLa wt cells. The cells were seeded in multi-well plates and culture until they became confluent. Once they became confluent, using a yellow pipette tip was performed a straight scratch, simulating a wound. At this point, the images were acquired at regular time interval by confocal microscopy.

Chapter4

Results

4.1 TFEB overexpression in different cell lines causes a drastical change in cell shape

The idea that TFEB could have a role in actin remodelling starts with the observation that in the condition of TFEB overexpression, different cell lines such as HeLa, U2OS, ARPE19 and COS7, show strong morphological changes in their shape (Fig. 7).

In order to detect F-actin, cells were stained with phalloidin after 48h for transfection with a construct coding TFEB fused to the GFP. In all the cell lines analyzed, I could observe the same phenotype: in TFEB overexpression condition, the shape of the cells was drastically changed when compared to the not transfected cells (control cells). In particular, I observed that in cells overexpressing TFEB-GFP, there was an increase in the numbers of filopodia-like structure outside the cells; structures that were almost absent in the control cells.

As shown in Fig. 7, in COS7 cells, that are commonly used to conduct studies in filopodia formation[113], after TFEB-GFP transfection I could observe the strongest phenotype in terms of the number of filopodia when compared to the control cells.

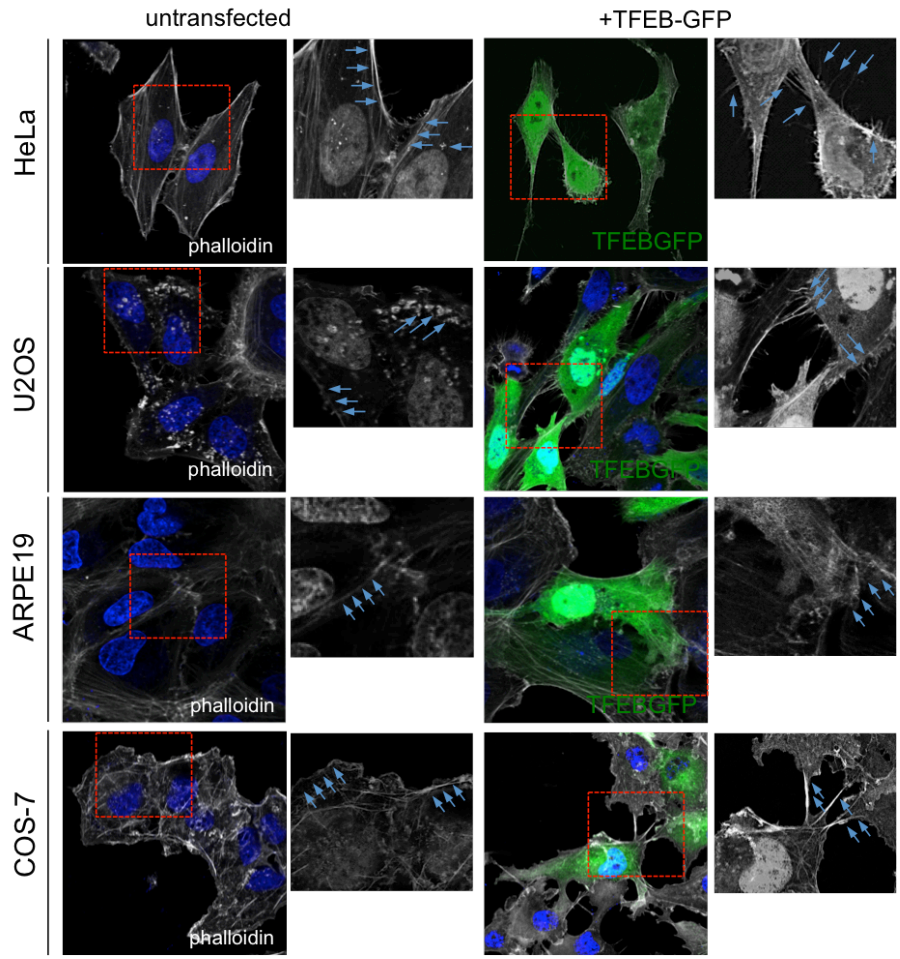

Fig. 7 Overexpression of TFEB WT in HeLa, U2OS, ARPE19 and COS7 cells induce morphological shape changes

Fluorescence analysis of untransfected cells compared to transfected cells with TFEB wt isoform. HeLa cell line (upper), U2OS cell line (second line), ARPE19 cell line (third line), COS7 (lower).

In blue DAPI: 4',6'-diamidino-2-phenylindole staining; in green EGFP: fused with TFEB wt isoforms; in grey: phalloidin dye against actin cytoskeleton.

Moreover, a wound healing assay using stable HeLa cell line overexpressing TFEB, revealed that one day after the generation of the wound, HeLa wt cells were not able to completely repair

the wound (Fig 8, upper panel); overexpressing TFEB HeLa cells, start to repair it 20 hours after the wound (Fig 8, lower panel).

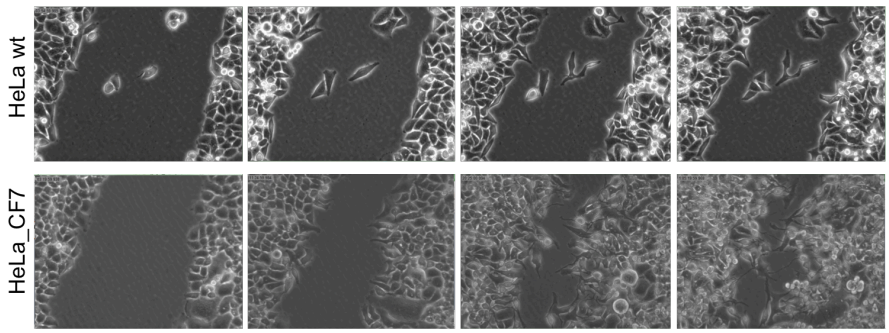

Fig. 8 TFEB overexpression increase the ability of cell migration
Wound Healing assay on HeLa wt cells and HeLa TFEB overexpressing stable clone (CF7); The cells are analyzed or 1day and the photograms are extrapolated by the movie.

From these preliminary observations, I started to investigate the new role of TFEB in regulating genes involved in actin remodeling and filopodia formation.

4.2 Bioinformatics analysis reveals the presence of CLEAR binding sites in the promoters of actin and filopodia related genes

To understand the TFEB involvement in actin remodeling and in filopodia initialization, elongation and regulation, I performed a bioinformatics analysis regarding the most important genes involved in filopodia network (Tab. 2). The website TFEB.tigem.it previously developed at the Telethon Institute of Genetics and

Medicine (TIGEM), was used to analyze the presence of CLEAR binding sites on the promoter of genes involved in the actin cytoskeleton remodeling and the filopodia network.

In this database are stored more than 20000 genes that could be potentially TFEB target genes.

From this interrogation, I generated a list of 10 genes (TAB. 2) that could be potentially regulated by TFEB and that are involved in the actin and filopodia related processes.

Name	Rank score	CLEAR BS	ChIP analysis
Cell division control protein42 CDC42	0.023287153	ch11 (-655; -629)	NO
Rho In Filopodia RIF	0.03667024	ch12 (-236)	NO
Actin-Related Protein-2 ARPc2	0.022912024	ch2 (-464)	NO
Actin-Related Protein-3 ARPc3	0.022194964	NO predic.CLEAR	NO
Wiskott-Aldrich Syndrome WASp	0.021260483	chX (-991; -481)	NO
WASP-family verprolin-homologous WAVE	0.060138207	NO predicted CLEAR	SI
Diaphanous-Related Formin-2 DIA2	0.022486424	NO predicted CLEAR	NO
Fascin FSCN1	0.057863838	ch7 (-649)	NO
Insulin-Receptor Substrate p53 IRSp53	0.73349526	ch17 (-486; -468; +72)	NO
Epidermal Growth Factor Receptor Pathway Substrate 8 EPS8	1.742853118	ch12(-748)	NO

TAB. 2 Bioinformatic analysis of filopodia network genes

In the table is reported the binding rank score, the presence or not of the CLEAR binding sites, and the positivity at ChIP analysis[13] of the principal genes involved in filopodia network.

4.3 TFEB activation causes an increase in mRNA level of filopodia genes in HeLa cell

As first experiments to validate this list of actin-filopodia related genes, I performed quantitative RT-PCR on mRNA extracted from HeLa cell overexpressing the TFEB wt isoform (wt-TFEB), the TFEB S142/211A constitutively active isoform (S142/211A-TFEB) and TFE3 wt isoform (wt-TFE3), using specific oligos for each gene (Fig. 9; see methods).

The qRT-PCR data revealed an increased mRNA level for two genes: EPS8 and IRSp53. These genes were, indeed, upregulated in the condition of overexpression of wt-TFEB, S142/211A-TFEB and wt-TFE3 when compared to the untransfected cells (Fig. 9).

EPS8 and IRSp53 are the most important genes involved in filopodia elongation, therefore these results were in agreement with the previous observation of an increased numbers of filopodia in cells overexpressing TFEB.

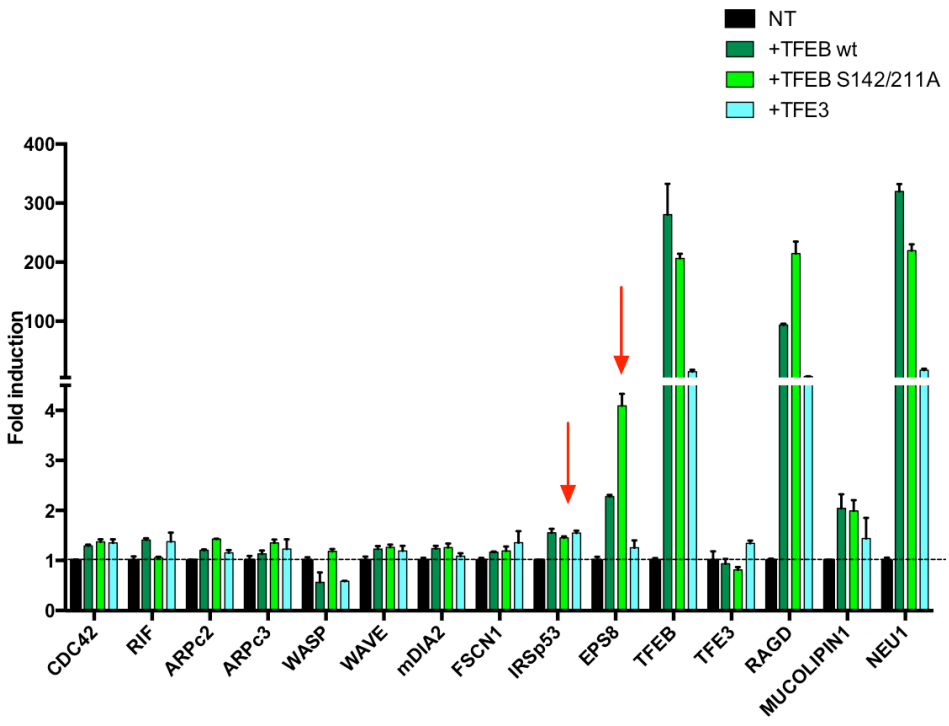

Fig. 9 RT-PCR of filopodia network genes

The qRT-PCR analysis was performed on the principal genes involved in filopodia formation pathway to evaluate the RNA levels in wt-TFEB, S142/211A-TFEB, wt-TFE3 overexpression. The cells were collected after 48h post-transfection.
RAGD, Mucolipin1, NEU1 are known TFEB gene target and are used as positive control.

As mentioned before, TFEB has a very tight regulation. It is activated by cellular stress or by starvation conditions; in these conditions, it migrates into the nucleus and is able to activate the transcription of its gene target. For this reason, I decided to analyze the regulation of endogenous TFEB levels, on IRSp53 and EPS8 in different starvation conditions.

To this end I performed qRT PCR experiments in two different starvation conditions; 1) total starvation, treating the cells with HBSS enriched with HEPES 10μM, and 2) amino acids starvation, treating the cells with RPMI media without amino acids and in absence of glutamine. By the qRT analysis, I could observe, that like for the canonical target genes of TFEB (RAGD, NEU and MCLN1), I was able to appreciate an increase of IRSp53 (4 times) and EPS8 (5 times) mRNA levels in both the two different starvation condition, when compared to the untreated cells (Fig. 10).

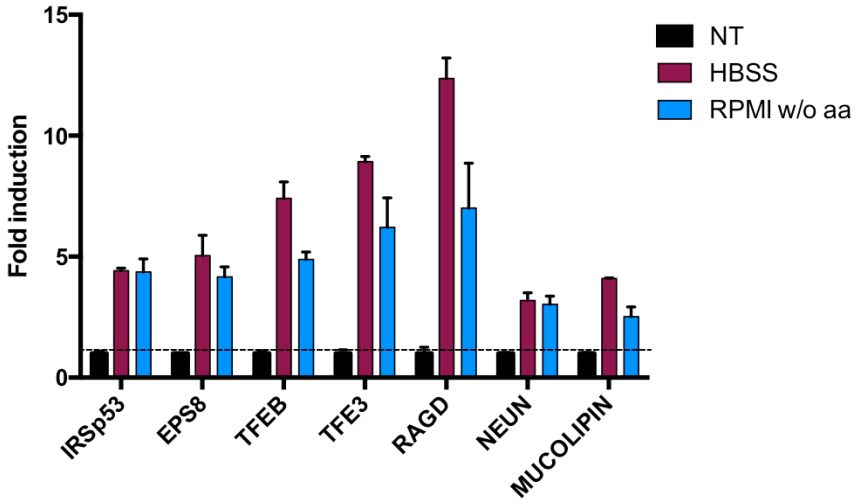

Fig. 10 Upregulation of filopodia genes upon HBSS and amino acid starvation

qRT-PCR analysis performed on IRSp53 and EPS8 in starvation condition. The cells starved with HBSS/Hepes 10μM were collected after 6h;

The cells starved with RPMI without amino acid were collected after 6h. RAGD, Mucolipin1, NEU1 are known TFEB gene target and are used as positive control.

4.4 TFEB depletion causes a decrease in mRNA level of EPS8 and IRSp53 genes in HeLa cell

To confirm that the increase of IRSp53 and EPS8 mRNA levels, in starvation condition was due to the TFEB/TFE3 activation, I decided to silence these two genes in HeLa cells and perform a qRT PCR experiment on mRNA extracted by control and TFEB and TFE3 silenced cells, in normal nutrient condition and after nutrient deprivation (starvation condition).

As expected, in control cells after HBSS and amino acid starvation treatments I could observe an increase in IRSp53 and

EPS8 mRNA level (Fig. 10). This increase was instead, undetectable in TFEB/TFE3 KD cells after HBSS starvation and amino acid starvation treatment (Fig. 11).

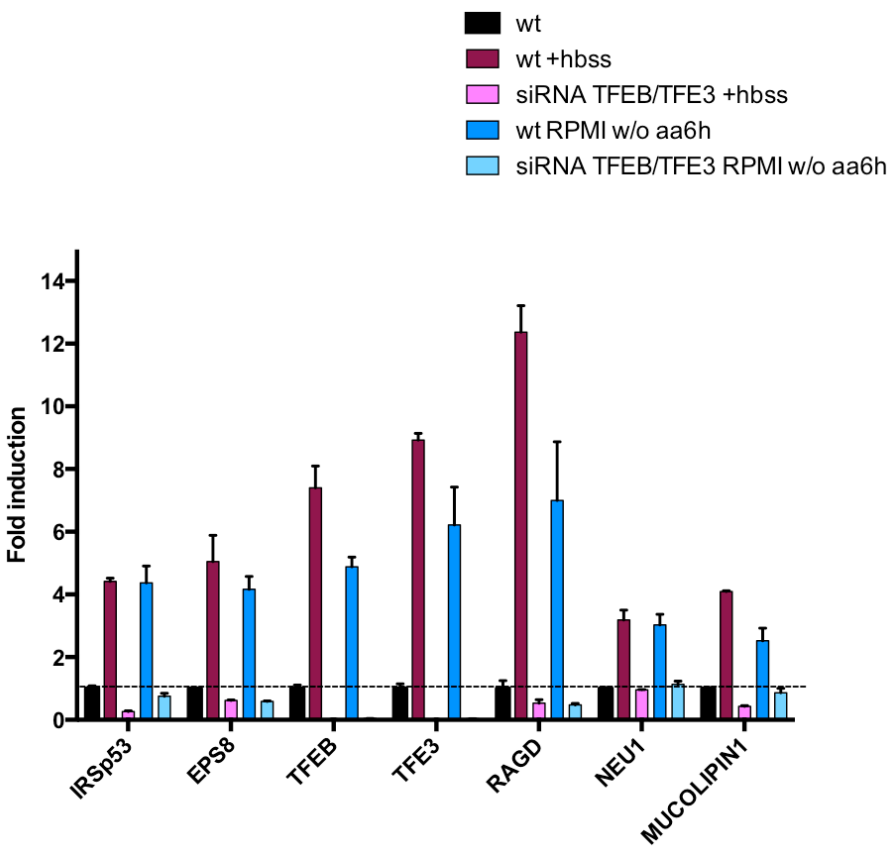

Fig. 11 Filopodia genes expression in KD TFEB-TFE3 HeLa cells

qRT-PCR analysis performed on IRSp53 and EPS8 in fed and starvation condition after 72h transfection with siRNA TFEB/TFE3. The cells starved with HBSS/Hepes 10mM were collected after 6h; The cells starved with RPMI without amino acid were collected after 6h; RAGD, Mucolipin1, NEU1 are known TFEB gene target and are used as positive control.

These qRT-PCR results indicate that IRSp53 and EPS8 show the same behaviour of the canonical TFEB/TFE3 target genes, which

upregulation is impaired in TFEB/TFE3 KD cells after starvation (Fig. 11).

Collectively these data strongly support the idea that IRSp53 and EPS8 can be potentially target genes of TFEB and TFE3, suggesting a role of these two transcriptions factor in regulating filopodia formation.

4.5 TFEB overexpression causes an increase in protein level of EPS8 and IRSp53 in HeLa cell

In order to establish a direct correlation between mRNA and protein levels of EPS8 and IRSp53 in a TFEB-dependent fashion, I decided to perform western blot (WB) experiments in HeLa cells overexpressing the TFEB-wt, TFEB S142/211A and TFE3-wt isoforms. After 48h of transfection, I collected the protein samples and I analyzed them with specific antibodies against EPS8 and IRSp53. As showed in Fig. 12, I could observe an increase of IRSp53 (second lane) and EPS8 (first lane) protein levels in cells transfected with wt-TFEB and S142/211A-TFEB, respectively, while the increased level of protein in the condition of TFE3 overexpression was observed only for the IRSp53 protein. The experiments were performed in triplicate and statistically validated (Fig12, right panel).

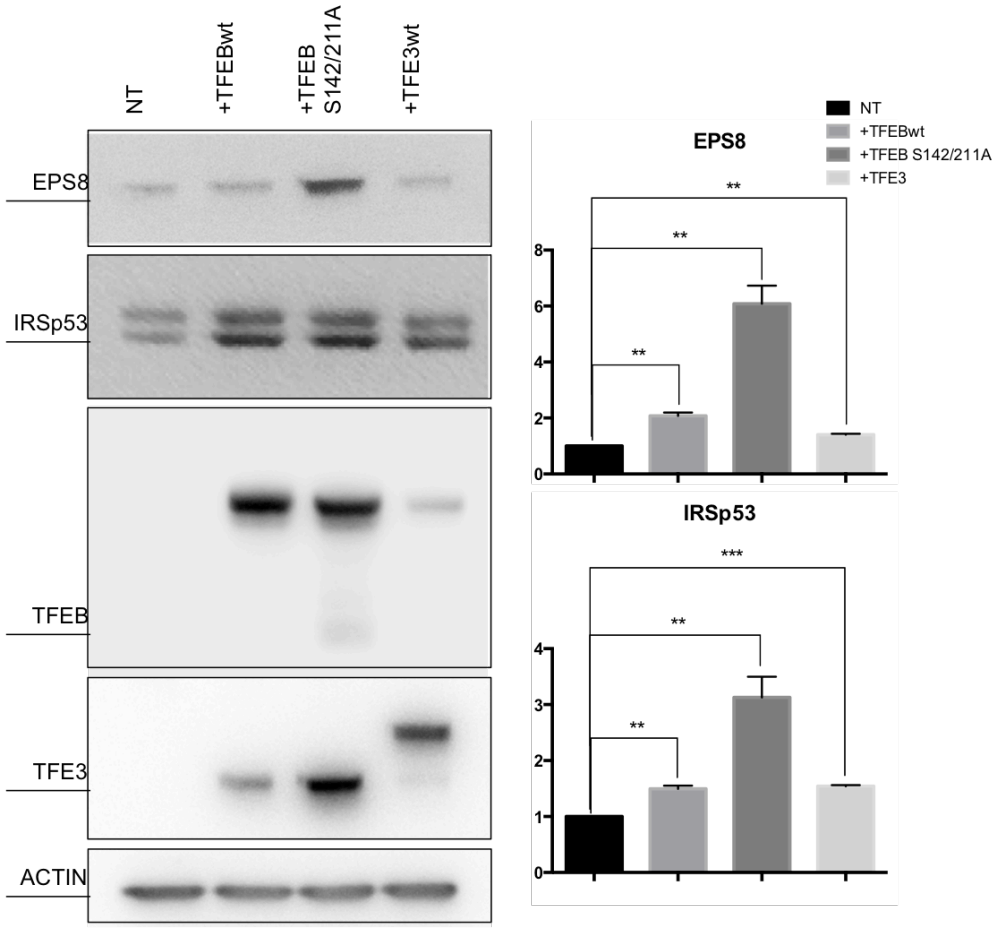

Fig. 12 Protein levels of EPS8, IRSp53 in overexpression condition HeLa cells

Immunoblot analyses performed on wt-TFEB, S142/211A-TFEB, wt-TFE3 transfected cells to evaluate the protein expression of filopodia network genes. Graphs represent the densitometry quantification of Western blot bands. Values are normalized to actin, and are shown as an average (± SEM) (* P <0.05, ** P < 0.01, *** P < 0.001, two-sided, Student's t-test).

Moreover, to follow the regulation of this protein in absence of TFEB and TFE3, I performed a WB experiment in HeLa cells depleted by siRNA of TFEB and TFEB/TFE3. As shown in Fig. 13, also in these experimental conditions I could detect a strong decrease of the EPS8 protein levels in absence of TFEB or

TFEB/TFE3, while the IRSp53 protein levels remain stable in all the experimental conditions (Fig. 13).

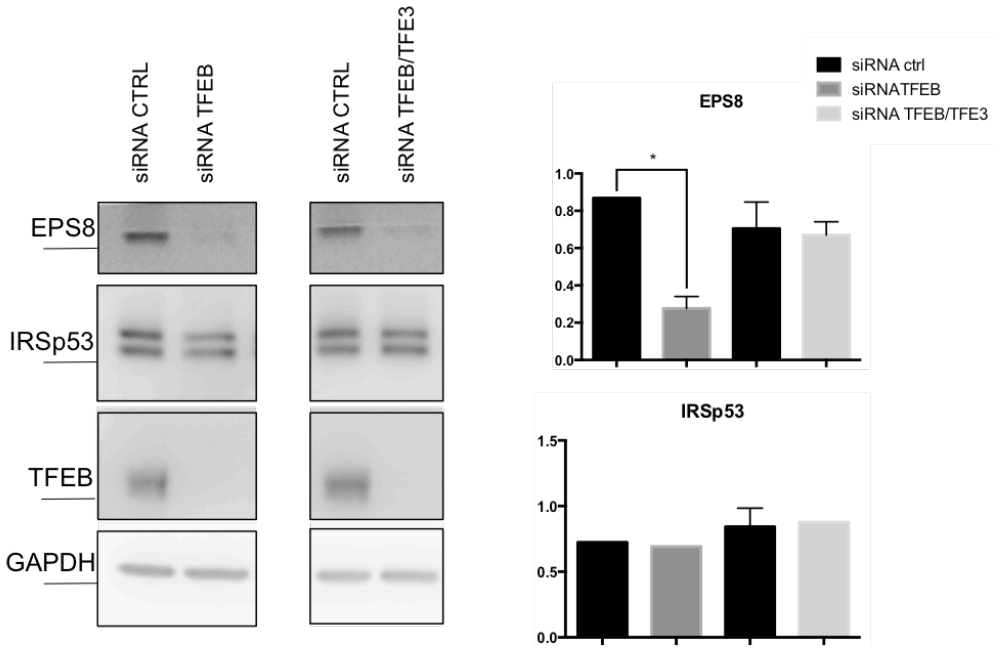

Fig. 13 Protein levels of EPS8, IRSp53 in HeLa cells TFEB KD

Immunoblot analyses performed on starved cells to evaluate the protein expression of filopodia network genes. The cells starved with HBSS/Hepes 10μM were collected after 6h; The cells starved with RPMI without amino acids were collected after 6h; Graphs represent the densitometry quantification of Western blot bands. Values are normalized to actin, and are shown as an average (± SEM) (* P <0.05, ** P < 0.01, *** P < 0.001, two-sided, Student's t-test).

This result suggests that the increase of mRNA level of IRSp53 and EPS8 in TFEB overexpressing conditions is closely linked to the increase of IRSp53 and EPS8 protein levels.

Instead, while EPS8 protein level decrease in absence of TFEB or TFEB and TFE3, the IRSp53 protein level seems to be more

stable in the same experimental conditions, suggesting that this two proteins could be differently regulated.

4.6 ChIP analysis of TFEB binding sites on filopodia promoters in HeLa TFEB overexpressing cells reveals a direct regulation of TFEB on EPS8

As showed in Table 2, the bioinformatics analysis of the genes involved in filopodia network, the IRSp53 gene promoter presents three different, non-canonical, CLEAR binding sites: one located at -489 bp (GTGCCA), the second one located at -468 bp (CACGCG) and the last one is located after the transcription start point and at +72 bp after +1 (Fig. 14).
The EPS8 gene promoter shows instead one canonical CLEAR binding site located at -748 bp (Fig. 14).

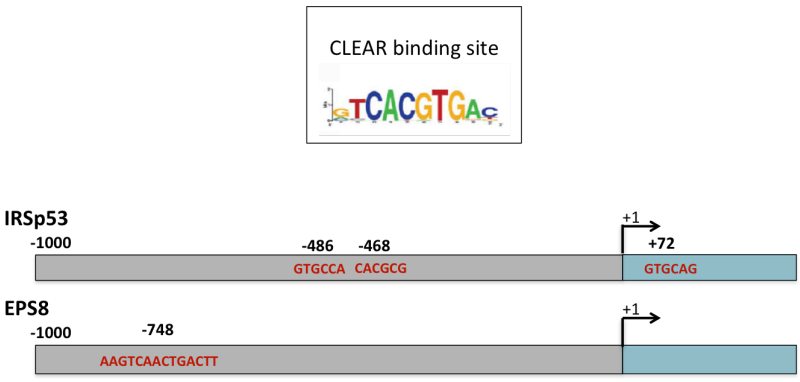

Fig. 14 Predicted CLEAR binding sites in IRSp53 and EPS8 genes
Schematic representation of IRSp53 and EPS8 promoters, and of the CLEAR binding sites present inside

Since the previous data strongly suggest a correlation between the TFEB and TFE3 activation and the regulation of the EPS8 and IRSp53 genes, I performed experiments of Chromatin Immunoprecipitation (ChIP) analysis in order to evaluate a direct binding of TFEB on the IRSp53 and EPS8 promoters.

To perform this experiment I used a stable cell line overexpressing TFEB fuse with a FLAG tag. To induce TFEB-FLAG activation I treated the cells with RPMI without amino acids.

To immunoprecipitate, TFEB-FLAG antibody against FLAG was used.

Coimmunoprecipitated samples were purified and analyzed by qRT-PCR. The results were analyzed in Fold Change of the target genes, IRSp53 and EPS8, in starved condition compared to the fed condition. ChIP analysis showed an enrichment of EPS8 in HeLa starved cells compared to untreated cells. This data is consistent and significant (Fig. 15).

Surprisingly, I could not find any enrichment for the IRSp53, suggesting that this gene, even if its expression seems to be regulated in the condition of TFEB overexpressing and during starvation, is not a direct target of TFEB (Fig. 15).

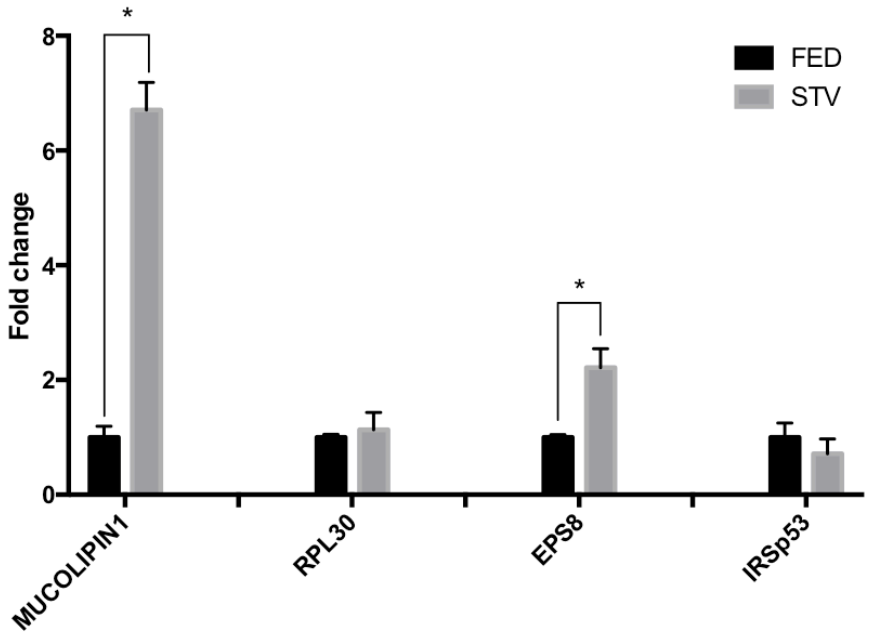

Fig.15 ChIP analysis on predicted CLEAR binding sites on filopodia genes
The graph represents the qPCR analysis performed on ChIP experiments on EPS8 and IRSp53 on a stable clone TFEB overexpressing cells starved by RPMI without amino acids then untreated cell.
The results are expressed in terms of Fold Change.
MUCOLIPIN1 represents the positive control; RPL30 represent the negative control.

On the other hand, ChIP assay experiments revealed that only EPS8 is a direct TFEB transcriptional target; since TFEB is able to recognize and bind the CLEAR binding site present on the EPS8 promoter. In turn, EPS8 overexpression is able to bind IRSp53, and together, they play a fundamental role in filopodia formation and elongation.

4.7 TFEB and TFE3 overexpression induce filopodia formation in HeLa cell

The drastic change in cell shape after TFEB overexpression, the increased ability of these cells to migrate, and the ability of TFEB to directly regulate the EPS8 gene, a master regulator of filopodia induction, strongly suggest that TFEB could play the main role in filopodia formation. In order to statistically confirm the effect on filopodia increase upon TFEB and TFE3 activation, I performed a quantitative analysis of immunofluorescence experiments using ImageJ software in order to count filopodia in different experimental condition. HeLa cells overexpressing wt-TFEB, S142-211A-TFEB and wt-TFE3 using were stained with phalloidin, an F-actin probe fluorescent dye, used to mark F-actin and MYOX antibody that recognizes and marks the final point of filopodia tips.

In normal nutrient condition, the cytoskeleton appears very smooth in some areas without any protrusions or with few filopodia, marked by MYOX (Fig. 16A).

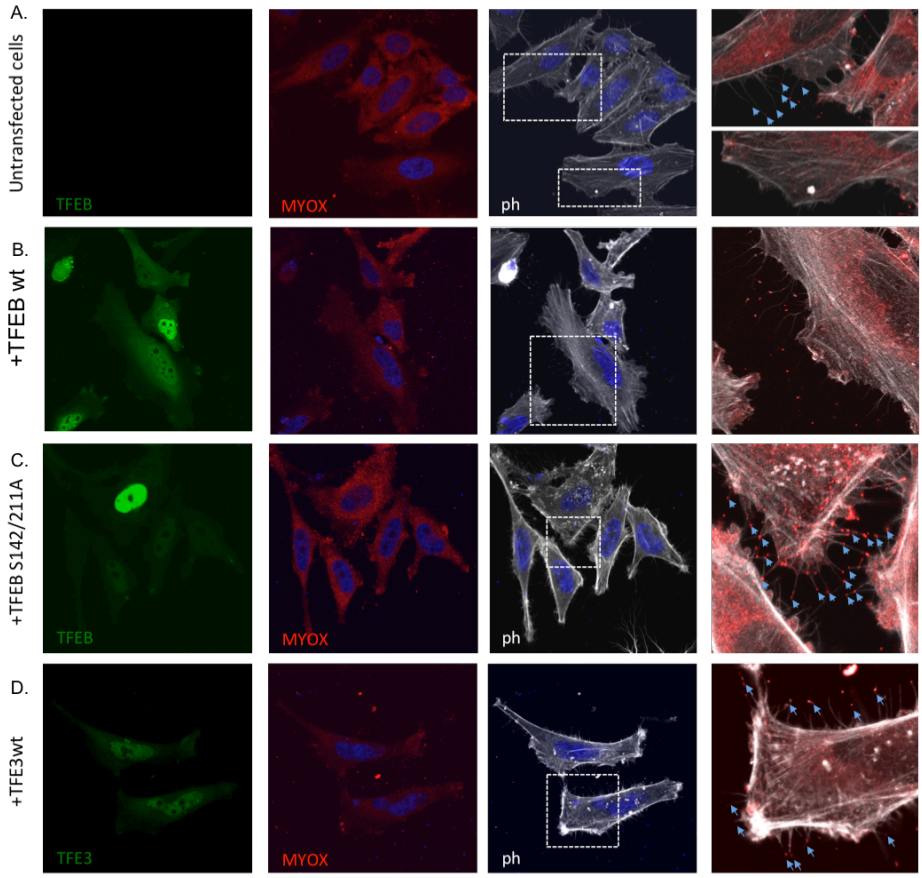
A.
Untransfected cells
TFEB
MYOX
ph
B.
+TFEB wt
C.
+TFEB S142/211A
TFEB
MYOX
ph
D.
+TFE3wt
TFE3
MYOX
ph

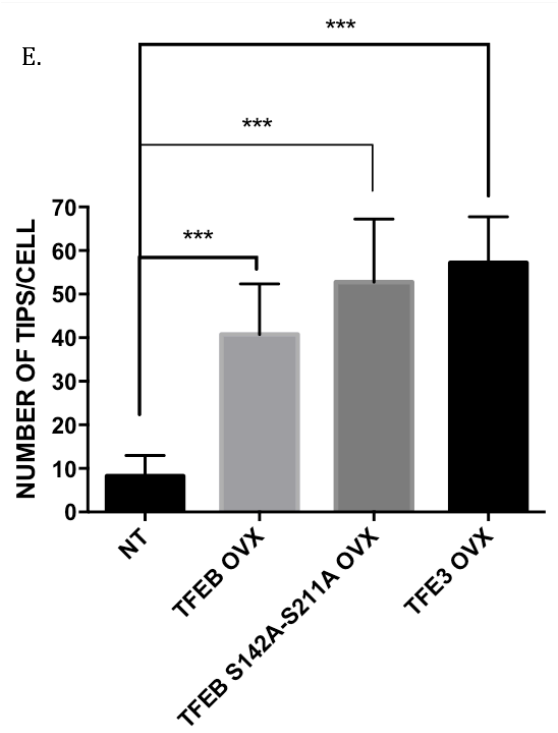
E.
***
***
***
NUMBER OF TIPS/CELL
70
60
50
40
30
20
10
0
NT
TFEB OVX
TFEB S142A-S211A OVX
TFE3 OVX

Fig. 16 Overexpression of WT-TFEB, S142/211A-TFEB and wt-TFE3 in HeLa cells induce an increase of MYOX tips

Fluorescence analysis of TFEB and MIOX in untransfected cells (A), the cell transfected with wt-TFEB (B), S142/211A-TFEB (C) and wt-TFE3 (D). In blue DAPI (4',6'-diamidino-2-phenylindole staining), in green EGFP fused with the two TFEB isoforms and with TFE3. In red: MYOX antibody staining. In grey: phalloidin dye against actin cytoskeleton.

E. The Number of filopodia in untransfected cell, the cell transfected with wt-TFEB, S142/211A-TFEB and wt-TFE3. The count was obtained analyzing the same number of images using Cell Counter the plugin of ImageJ program and was normalized to untransfected cells (E). The values are shown as an average (± SEM) (* P <0.05, ** P < 0.01, *** P < 0.001, two-sided, Student's t-test).

As shown in Fig.16, since the wt-TFEB expression levels are high, TFEB translocates into the nucleus, where it can activate filopodia genes. In these conditions, I could appreciate an increase in filopodia number (Fig.16 A-E).

As expected, in cells transfected with S142/211A-TFEB, the constitutive active isoform, I could observe the same phenotype (Fig. 16C-E), as well as, in cells transfected with TFE3 I was able to count more filopodia when compared to the untransfected cells (Fig. 16D-E).

Using ImageJ software I could count the number of filopodia *per* cell. The results are reported in Fig 16E.

I found that the filopodia number in the cells transfected with the wt-TFEB or the S142/211A-TFEB was 4 and 5 times higher than the number counted in normal nutrient condition, respectively.

The same results were obtained counting filopodia in cells transfected with wt-TFE3.

4.8 TFEB and TFE3 activation regulates filopodia formation in HeLa cell

In order to establish the role of TFEB and TFE3 in regulating filopodia formation, I also performed experiments of immunofluorescence with MYOX, in nutrient deprivation condition (starvation) to induce TFEB and TFE3 activation. In starvation condition, after treatment with HBSS/Hepes 10μM, I could detect a strong increase in filopodia number marked by MYOX, if compared with the untreated cell (Fig. 17B, A).

I could also observe a more dramatic effect on filopodia number increase after treatment with RPMI without amino acids (Fig. 17C).

To confirm that the filopodia induction was directly regulated by TFEB and TFE3 activation, I performed the same experiments on cells TFEB and/ or TFE3 depleted.

In normal nutrient condition, TFEB depleted cells appears drastically different compared to control cells, showing a total absence of filopodia (Fig. 17D).

The presence of filopodia was then investigated in the cell with TFEB depleted but in starvation condition. In absence of TFEB, under the starvation condition, cells are not able to induce filopodia (Fig. 17E). I could observe the same phenotype in

condition of starvation performed using amino acids depletion (Fig. 17F).

Moreover, I could observe the absence of filopodia in cells depleted of both TFEB and TFE3 under normal nutrient condition (Fig. 17G) and starvation condition (Fig. 17H, I). These results confirm that the increase of filopodia number, observed in starvation condition, was due to the TFEB and TFE3 activation. The images have been quantified and statistically validated by T-test Fig. 17 L.

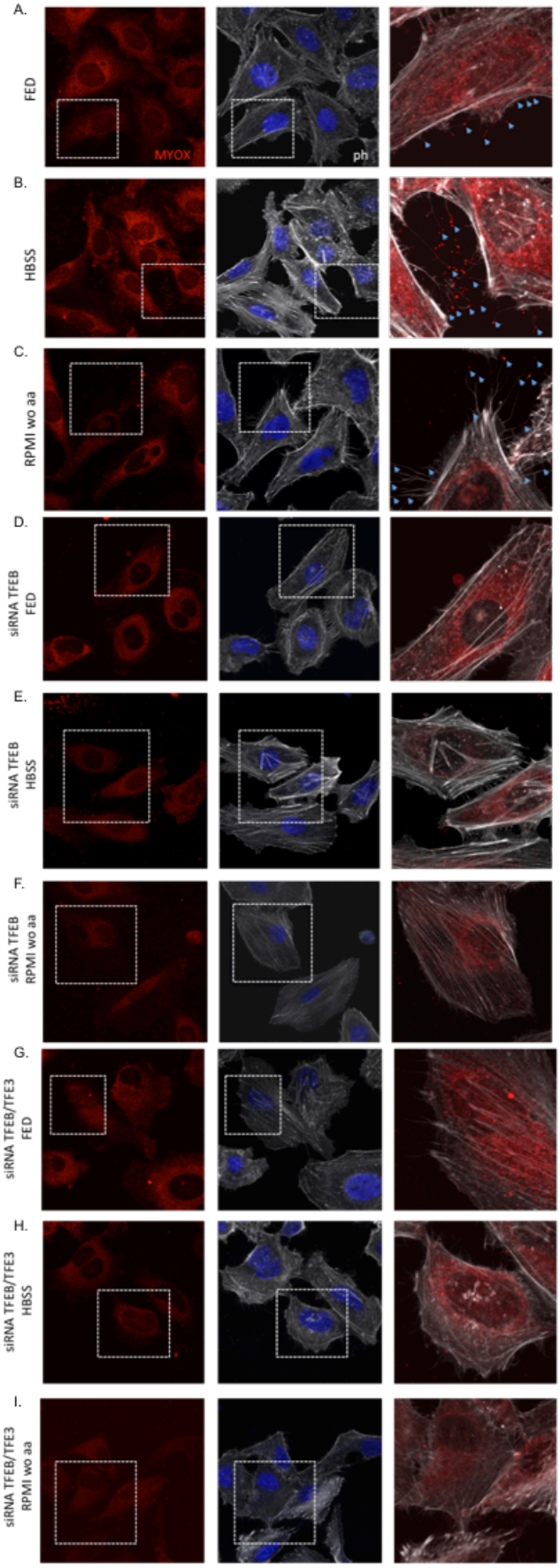
A.
FED
MYOX
ph
B.
HBSS
C.
RPMI wo aa
D.
siRNA TFEB
FED
E.
siRNA TFEB
HBSS
F.
siRNA TFEB
RPMI wo aa
G.
siRNA TFEB/TFE3
FED
H.
siRNA TFEB/TFE3
HBSS
I.
siRNA TFEB/TFE3
RPMI wo aa

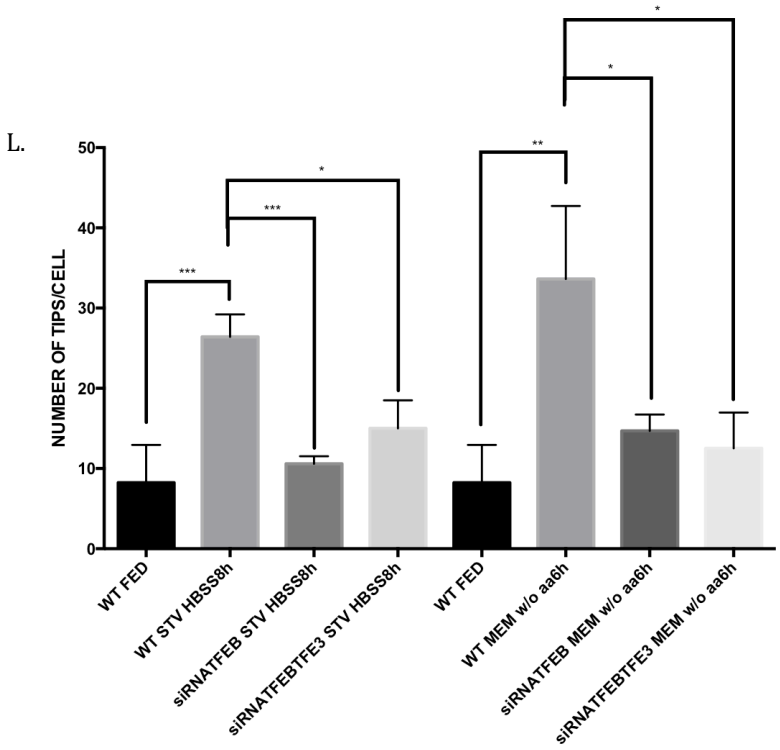

Fig. 17 TFEB nuclear translocation upon HBSS and amino acids starvation in HeLa cells induces an increase of MYOX marked tips; The absence of TFEB and TFEB/TFE3 together, upon HBSS and amino acids starvation in HeLa cells causes a decrease of MYOX marked tips

Fluorescence analysis of wt fed cells (line A), HeLa wt starved cells with HBSS/Hepes 10mM (line B), HeLa wt starved cells with RPMI without amino acids (line C), TFEB KD cells in normal nutrient condition (line D), TFEB KD starved cells with HBSS/Hepes 10μM (line E), TFEB KD starved cells with RPMI without amino acids (line F), TFEB/TFE3 KD fed cells (line G), TFEB/TFE3 KD starved cells with HBSS/Hepes 10μM (line H), TFEB/TFE3 KD starved cells with RPMI without amino acids (line I). L. Number of filopodia per cell is reported. The values are shown as an average (± SEM) (* $P < 0.05$, ** $P < 0.01$, *** $P < 0.001$, two-sided, Student's t-test).

To confirm that the mechanism, by which TFEB regulates the formation of filopodia after starvation, is through the activation

of EPS8 and IRSp53, I performed immunofluorescence experiments of MYOX and F-actin in cells depleted of IRSp53 and EPS8. As expected, after starvation by HBSS/Hepes 10μM (Fig. 18B) and RPMI without amino acids (Fig.18C), in HeLa wt cells, TFEB migrates into the nucleus and the cells shown more filopodia compared to untreated cells (Fig. 18A, B, C). In IRSp53/EPS8 KD cells, after HBSS/Hepes 10μM (Fig. 18D) and RPMI without amino acids (Fig.18E) starvation, although TFEB migrates into the nucleus, the cells are not more able to form filopodia and the cytoskeleton appears very rarefied and cloudy.

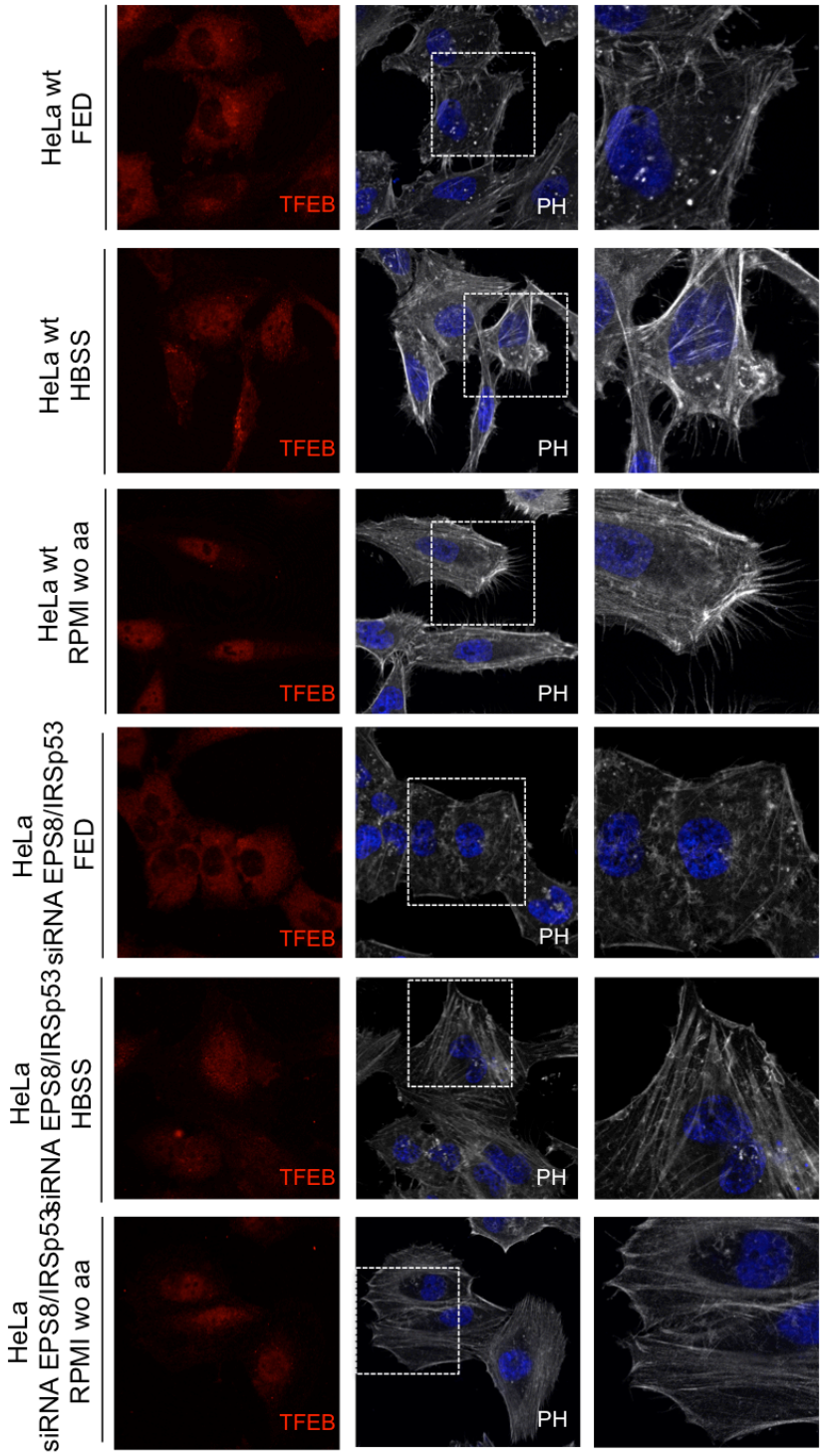
HeLa wt FED
HeLa wt HBSS
HeLa wt RPMI wo aa
HeLa siRNA EPS8/IRSp53 FED
HeLa siRNA EPS8/IRSp53 HBSS
HeLa siRNA EPS8/IRSp53 RPMI wo aa
TFEB
PH

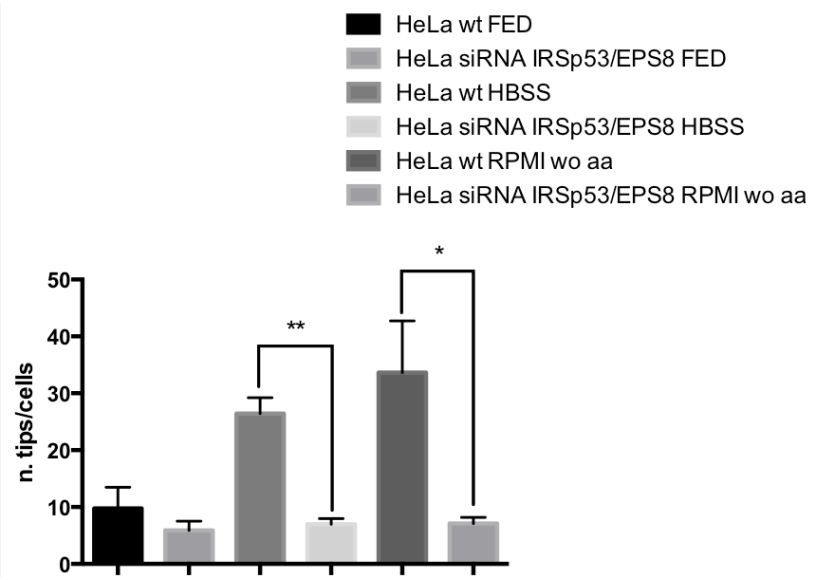

Fig. 18 The absence of IRSp53 and EPS8 prevents the filopodia formation under starvation treatments in HeLa cells

Fluorescence analysis of HeLa wt fed cells (line A), HeLa wt starved cells with HBSS/Hepes 10μM (line B), HeLa wt starved cells with RPMI without amino acids (line C), IRSp53/EPS8 KD fed cells (line D), IRSp53/EPS8 KD starved cells with HBSS/Hepes 10μM (line E), IRSp53/EPS8 KD starved cells with RPMI without amino acids (line F).
In blue DAPI: 4',6'-diamidino-2-phenylindole staining; In red: TFEB antibody against the endogenous protein. In grey: phalloidin dye against actin cytoskeleton.

4.9 Melanoma Cell line shows an increase in mRNA and protein levels of IRSp53 and EPS8

IRSp53/EPS8 complex plays an important role in the positive regulation of cancer cell motility and invasiveness in metastatic tumor cell line[24]. These genes are, indeed, overexpressed in

tumor cell line. According to my results, this overexpression could be due to an upregulation of TFEB and TFE3.

To test this hypothesis I decided to investigate the level of EPS8 and IRSP53 in melanoma cell line, in particular, I choose the 501Mel cells, a specific cell line[25], associated with high levels of MITF, another member of the MiT/TFE family. By qRT experiments I could observe that the IRSp53 and EPS8 transcription levels in 501Mel are upregulated at about 2 and 2.5 times, compared to control cell line P375A (Fig. 19). More important, in the same cell line but depleted of MITF or TFEB/TFE3, I could observe a reduction of the transcription levels of IRSp53 and EPS8 when compared to control cells (Fig. 19).

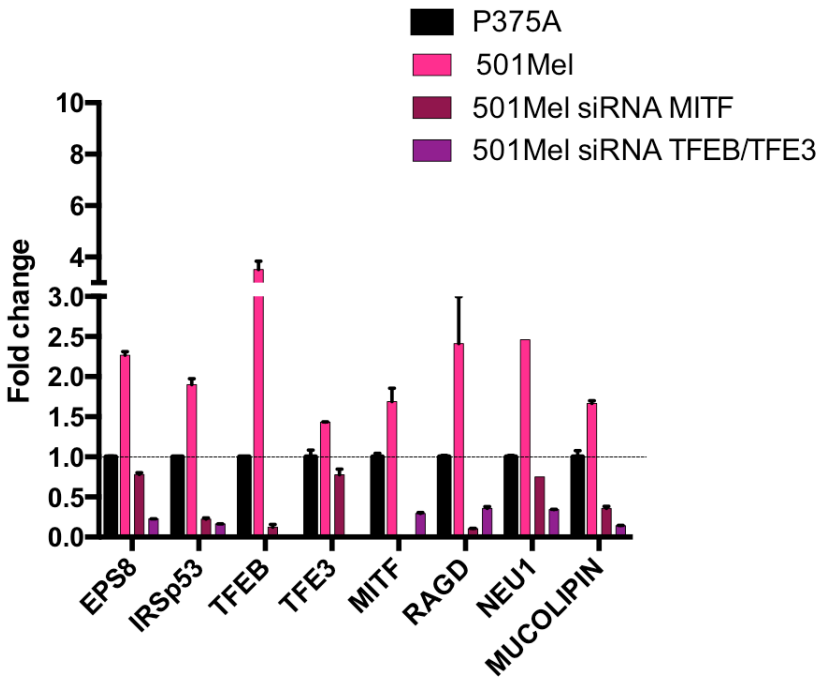

Fig. 19 Upregulation of filopodia genes in Melanoma cells

RT-PCR analysis performed on IRSp53, EPS8 and MYOX to evaluate the RNA levels in 501Mel cell line than to CTRL cells, MITF KD 501Mel cells and TFEB/TFE3 KD 501Mel cells.
The cells were collected after 72h post-transfection.

As expected, IRSp53 and EPS8 protein levels have the same trend.

In 501Mel, IRSp53 and EPS8 protein level increase of 1.5 times, for both, compared to control cells (Fig. 20).

A reduction of IRSp53 was also observed in cell depleted of MITF or TEFB and TFE3 (Fig. 20). Western blot experiments were performed in triplicate and statistically validated.

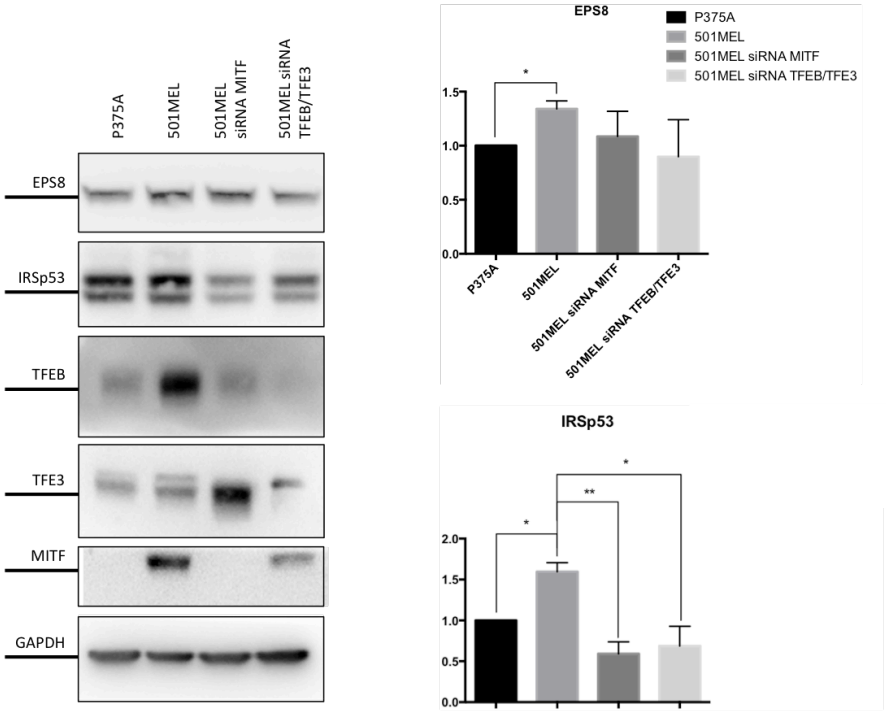

Fig. 20 Protein levels of EPS8, IRSp53 in 501Mel cells

Immunoblot analyses performed on IRSp53 and EPS8 to evaluate the protein levels in 501Mel cell line, MITF KD 501Mel cells and TFEB/TFE3 KD 501Mel cells.
The cells were collected after 72h post-transfection. Data are shown as the average (± SEM) of three different experiments and values are normalized to the untransfected cells (* P <0.05, ** P < 0.01, *** P < 0.001, two-sided Student's t-test).

4.10 Filopodia number is increased in Melanoma cell line

I decided to analyze the presence of filopodia in 501-Mel cell line. To this end, immunofluorescence experiments were analyzed by imageJ software in order to count filopodia marked by MYOX antibody in 501-Mel and in control cells (P375A).
Results are showed in Fig. 21, filopodia number is increased in 501Mel cells compared to control cells (P375A), in normal nutrient condition; while after depletion of MITF or TFEB/TFE3, the filopodia phenotype was totally rescued and the 501-Mel cells became more similar to the control cells (Fig. 21).

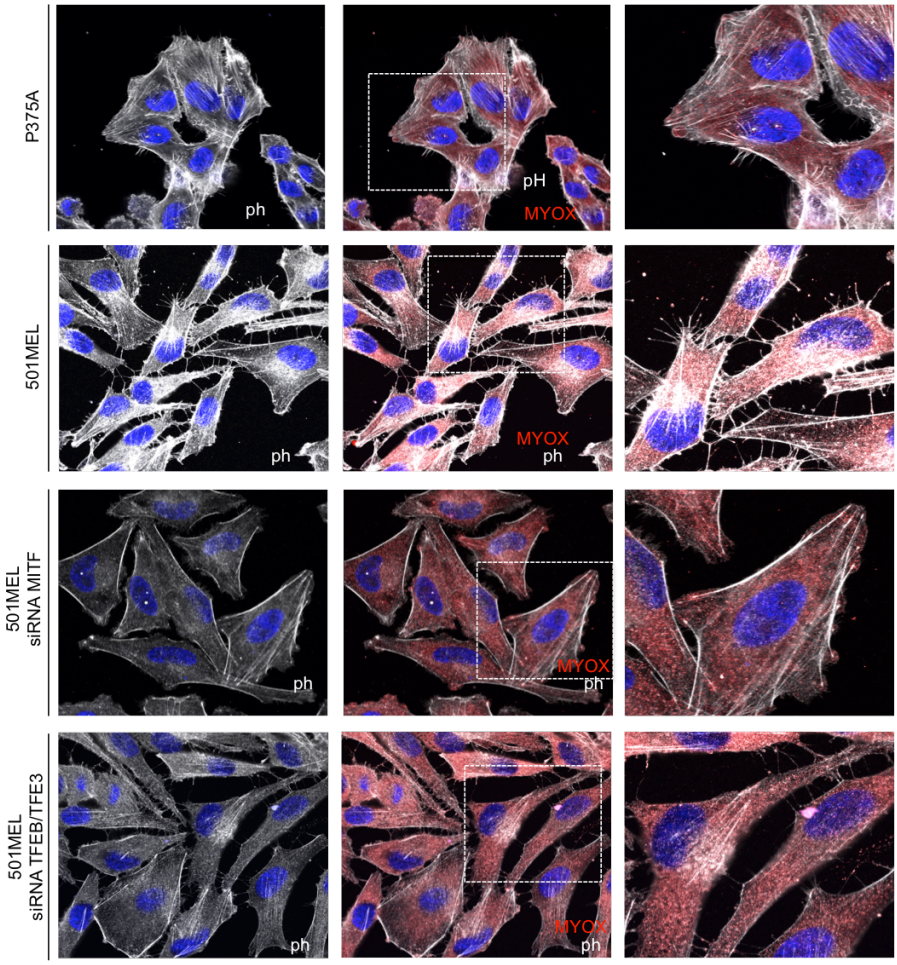
P375A
501MEL
501MEL siRNA MITF
501MEL siRNA TFEB/TFE3
ph
pH
MYOX

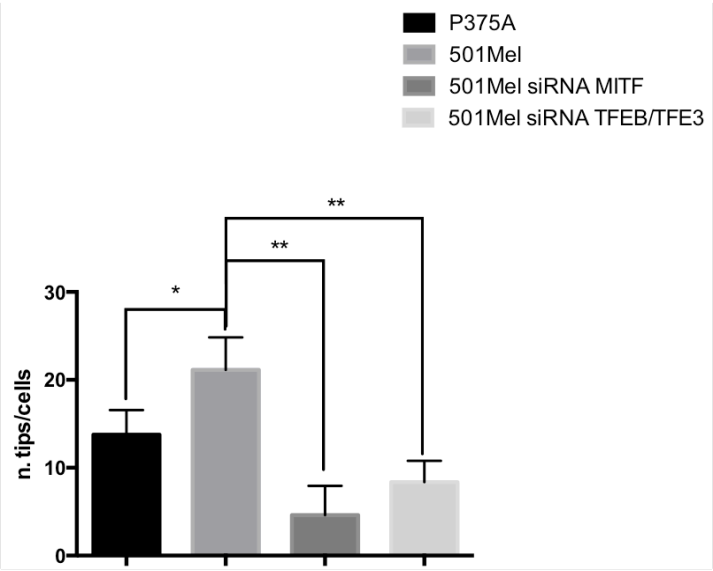
P375A
501Mel
501Mel siRNA MITF
501Mel siRNA TFEB/TFE3
n. tips/cells
0
10
20
30
*
**
**

Fig. 21 Upregulation of MITF in Melanoma cells induces an increase of MYOX tips

Fluorescence analysis CTRL (line A), 501Mel (line B), and MITF KD 501Mel cells (line C), TFEB/TFE3 KD 501Mel cells (line D); In blue DAPI: 4',6'-diamidino-2-phenylindole staining; In red: MYOX antibody against the protein. In grey: phalloidin dye against actin cytoskeleton.

Values graph are shown as an average (± SEM) (* P <0.05, ** P < 0.01, *** P < 0.001, two-sided, Student's t test).

4.11 TFEB overexpression in HeLa stable cell line increases the invasiveness ratio of the cells

All the data produced in this thesis work, demonstrate that TFEB and TFE3 have a key role in filopodia formation, regulating indirectly or directly two genes involved in filopodia network, IRSp53 and EPS8.

The abundance of filopodia at the leading edge of the cells is considered as a characteristic of invasiveness in the cancer cell and, moreover, filopodia are directly connected to cell migration because all components involved in filopodia formation are fundamental to cell motility.

For this reason, I decided to investigate if TFEB and TFE3 could have a role in increasing cell invasiveness.

Invasion through the extracellular matrix (ECM) is an important step in tumor metastasis. Cancer cells initiate invasion by adhering and spreading along the blood vessel wall. Proteolytic enzymes, such as MMP collagenases, dissolve tiny holes in the

sheath-like covering surrounding the blood vessels to allow cancer cells to invade[114,115].

I decided to use the CHEMICON cell invasion assay kit that is ideal for evaluation of invasive tumor cells.

I evaluated the invasive ratio of TFEB overexpressing HeLa stable clone (CF7) compared to HeLa control cell line.

48h after plating the cells, TFEB overexpressing cells are double in the lower part of the chamber membrane than to control cell (Fig. 22), indicating that in the same conditions, the cells overexpressing TFEB have a double invasive power compared to control cells.

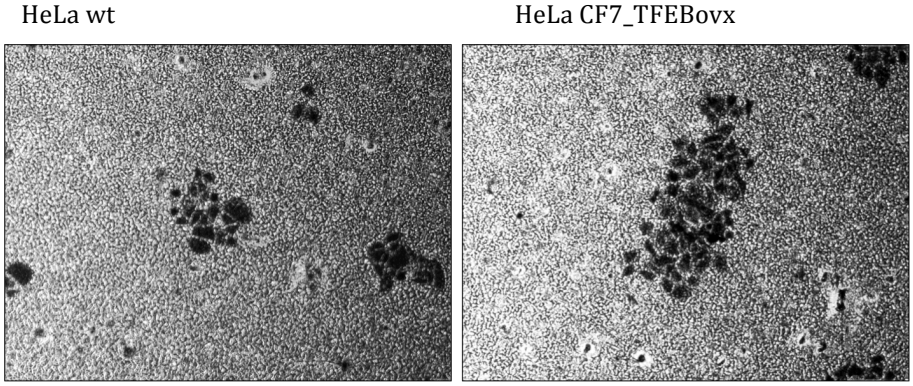

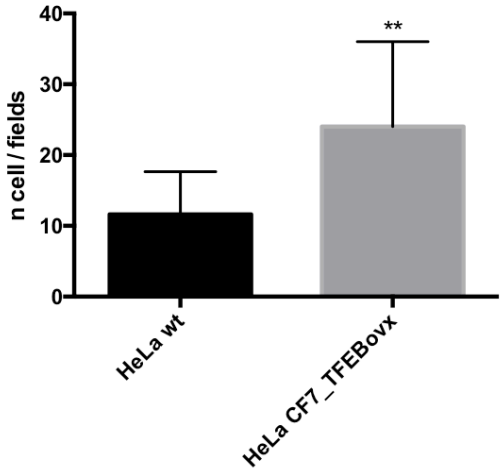

Fig. 22 TFEB overexpression increases the ability of invasiveness of the cells

Invasion assay on HeLa wt cells and HeLa stable clone TFEB overexpressing (CF7) cell; The cells are analyzed after 48h plating in the same specific chamber and are photographed by APOTOME microscope. The count is done on the same number of images, using ImageJ program, Cell Counter plugin, the values are shown as an average (± SEM) (* P <0.05, ** P < 0.01, *** P < 0.001, two-sided, Student's t-test).

These results are in agreement with the wound-healing assay, and strongly support a role of TFEB in contributing in cells migration and invasiveness regulating the formation and elongation of filopodia, through the transcriptional activation of EPS8 and IRSp53.

Chapter 5

Discussion

TFEB has been shown to be a master regulator of lysosomal biogenesis, function and autophagy, via transcriptional control of gene expression. In the last years, several studies have elucidated the mechanism of TFEB regulation, showing the existence of a lysosome-to-nucleus signaling mechanism that senses environmental changes and regulates lysosomal function via TFEB phosphorylation. Moreover, TFEB roles have been associated in tumorigenesis in different tissues, although the specific genes involved and the associated mechanisms are still unclear.

Filopodia are described as the sensor of the cell's surroundings and have been demonstrated to be important in cell motility. In turn, cell motility is involved at every stage of tumorigenesis and contributes to primary tumour growth, cancer cell dissemination and metastasis formation.

The discoveries of TFEB, as an important player in the formation and regulation of filopodia, could open a new view by which TFEB, through a transcriptional regulatory mechanism enables cellular adaptation to external cues and in physiopathological condition could contributes not only to the energetic metabolism of cancer cells, but also to a mechanistic point of view increasing cell motility.

From these studies, I demonstrate that two major genes, EPS8 and IRSp53, involved in filopodia formation, are regulated by TFEB and TFE3.

I revealed that in the condition of TFEB and TFE3 overexpression or overactivation the number of filopodia increases, while in a TFEB/TFE3 KD context they are totally absent. The increased number of filopodia correlates with the increased level of EPS8 and IRSP53 in TFEB/TFE3 overexpression condition as well as in the condition of TFEB/TFE3 activation under nutrient deprivation. Moreover, the upregulation of these genes upon nutrient deprivation disappears in the condition of TFEB/TFE3 KD, indicating that the regulation of these genes is mediated by TFEB and TFE3. As expected depletion of EPS8 and IRSP53, drastically reduce the number of filopodia in HeLa cell line under nutrient deprivation. ChiP data revealed that only EPS8 is a direct target of TFEB, suggesting that the regulation of IRSp53 could be due to an indirect effect on TFEB in regulating EPS8. Indeed, it has been demonstrated that IRSp53 is the principal partner of EPS8 in various cancer cell line and that the IRSp53/EPS8 complex occurs, at the leading edge of the cells, for motility and invasiveness[116].

To show the relevance of the TFEB/TFE3-EPS8 axis I decided to use a model of a cancer cell with the high level of invasiveness. Melanoma cell line was the best model to use, since the presence of high level of MITF at steady state that is required for melanoma proliferation. In this cell the number of filopodia, marked by MYOX increase drastically, as well as the mRNA and protein levels of IRSp53 and EPS8 compared to a control cell. Moreover, the increased number of filopodia was reduced in

absence of MITF as well as in the condition of TFEB and TFE3 depletion. Taking together these results, strongly suggest that TFE transcription factors play a key role in the regulation of filopodia formation.

Filopodia and filopodia proteins give a very critical contribution to cancer metastasis, the understanding of the pathophysiological processes underlying the role of filopodia in cancer could open a new attraction for therapeutic targets to block cancer dissemination. My data support the new idea that activation of TFEB could contribute to this mechanism and that acting on TFEB regulation could represent an effective strategy to rescue pathological conditions of metastases movement in cancer.

References

1 Steingrimsson, E., Copeland, N. G. & Jenkins, N. A. Melanocytes and the microphthalmia transcription factor network. *Annu Rev Genet* 38, 365-411, doi:10.1146/annurev.genet.38.072902.092717 (2004).

2 Beckmann, H., Su, L. K. & Kadesch, T. TFE3: a helix-loop-helix protein that activates transcription through the immunoglobulin enhancer muE3 motif. *Genes Dev* 4, 167-179 (1990).

3 Sato, S. *et al.* CBP/p300 as a co-factor for the Microphthalmia transcription factor. *Oncogene* 14, 3083-3092, doi:10.1038/sj.onc.1201298 (1997).

4 Zhao, G. Q., Zhao, Q., Zhou, X., Mattei, M. G. & de Crombrugghe, B. TFEC, a basic helix-loop-helix protein, forms heterodimers with TFE3 and inhibits TFE3-dependent transcription activation. *Mol Cell Biol* 13, 4505-4512 (1993).

5 Hemesath, T. J. *et al.* microphthalmia, a critical factor in melanocyte development, defines a discrete transcription factor family. *Genes Dev* 8, 2770-2780 (1994).

6 Aksan, I. & Goding, C. R. Targeting the microphthalmia basic helix-loop-helix-leucine zipper transcription factor to a subset of E-box elements in vitro and in vivo. *Mol Cell Biol* 18, 6930-6938 (1998).

7 Pogenberg, V. *et al.* Restricted leucine zipper dimerization and specificity of DNA recognition of the melanocyte master

regulator MITF. *Genes Dev* 26, 2647-2658, doi:10.1101/gad.198192.112 (2012).

8 Hallsson, J. H. *et al.* The basic helix-loop-helix leucine zipper transcription factor Mitf is conserved in Drosophila and functions in eye development. *Genetics* 167, 233-241 (2004).

9 Rehli, M., Den Elzen, N., Cassady, A. I., Ostrowski, M. C. & Hume, D. A. Cloning and characterization of the murine genes for bHLH-ZIP transcription factors TFEC and TFEB reveal a common gene organization for all MiT subfamily members. *Genomics* 56, 111-120, doi:10.1006/geno.1998.5588 (1999).

10 Bouche, V. *et al.* Drosophila Mitf regulates the V-ATPase and the lysosomal-autophagic pathway. *Autophagy* 12, 484-498, doi:10.1080/15548627.2015.1134081 (2016).

11 Pu, J., Guardia, C. M., Keren-Kaplan, T. & Bonifacino, J. S. Mechanisms and functions of lysosome positioning. *J Cell Sci* 129, 4329-4339, doi:10.1242/jcs.196287 (2016).

12 Ballabio, A. The awesome lysosome. *EMBO Mol Med* 8, 73-76, doi:10.15252/emmm.201505966 (2016).

13 Settembre, C., Fraldi, A., Medina, D. L. & Ballabio, A. Signals from the lysosome: a control centre for cellular clearance and energy metabolism. *Nat Rev Mol Cell Biol* 14, 283-296, doi:10.1038/nrm3565 (2013).

14 Settembre, C. & Medina, D. L. TFEB and the CLEAR network. *Methods Cell Biol* 126, 45-62, doi:10.1016/bs.mcb.2014.11.011 (2015).

15 Sardiello, M. *et al.* A gene network regulating lysosomal biogenesis and function. *Science* 325, 473-477, doi:10.1126/science.1174447 (2009).

16 Palmieri, M. *et al.* Characterization of the CLEAR network reveals an integrated control of cellular clearance pathways. *Hum Mol Genet* 20, 3852-3866, doi:10.1093/hmg/ddr306 (2011).

17 Settembre, C. *et al.* TFEB links autophagy to lysosomal biogenesis. *Science* 332, 1429-1433, doi:10.1126/science.1204592 (2011).

18 Medina, D. L. *et al.* Transcriptional activation of lysosomal exocytosis promotes cellular clearance. *Dev Cell* 21, 421-430, doi:10.1016/j.devcel.2011.07.016 (2011).

19 Napolitano, G. & Ballabio, A. TFEB at a glance. *J Cell Sci* 129, 2475-2481, doi:10.1242/jcs.146365 (2016).

20 Settembre, C. *et al.* A lysosome-to-nucleus signalling mechanism senses and regulates the lysosome via mTOR and TFEB. *EMBO J* 31, 1095-1108, doi:10.1038/emboj.2012.32 (2012).

21 Martina, J. A., Chen, Y., Gucek, M. & Puertollano, R. MTORC1 functions as a transcriptional regulator of autophagy by preventing nuclear transport of TFEB. *Autophagy* 8, 903-914, doi:10.4161/auto.19653 (2012).

22 Roczniak-Ferguson, A. *et al.* The transcription factor TFEB links mTORC1 signaling to transcriptional control of lysosome

homeostasis. *Sci Signal* 5, ra42, doi:10.1126/scisignal.2002790 (2012).

23 Sancak, Y. *et al.* Ragulator-Rag complex targets mTORC1 to the lysosomal surface and is necessary for its activation by amino acids. *Cell* 141, 290-303, doi:10.1016/j.cell.2010.02.024 (2010).

24 Sancak, Y. *et al.* The Rag GTPases bind raptor and mediate amino acid signaling to mTORC1. *Science* 320, 1496-1501, doi:10.1126/science.1157535 (2008).

25 Zoncu, R. *et al.* mTORC1 senses lysosomal amino acids through an inside-out mechanism that requires the vacuolar H(+)-ATPase. *Science* 334, 678-683, doi:10.1126/science.1207056 (2011).

26 Martina, J. A. & Puertollano, R. Rag GTPases mediate amino acid-dependent recruitment of TFEB and MITF to lysosomes. *J Cell Biol* 200, 475-491, doi:10.1083/jcb.201209135 (2013).

27 Medina, D. L. *et al.* Lysosomal calcium signalling regulates autophagy through calcineurin and TFEB. *Nat Cell Biol* 17, 288-299, doi:10.1038/ncb3114 (2015).

28 Settembre, C. *et al.* TFEB controls cellular lipid metabolism through a starvation-induced autoregulatory loop. *Nat Cell Biol* 15, 647-658, doi:10.1038/ncb2718 (2013).

29 Martina, J. A. *et al.* The nutrient-responsive transcription factor TFE3 promotes autophagy, lysosomal biogenesis, and clearance of cellular debris. *Sci Signal* 7, ra9, doi:10.1126/scisignal.2004754 (2014).

30 Ugurel, S. *et al.* Microphthalmia-associated transcription factor gene amplification in metastatic melanoma is a prognostic marker for patient survival, but not a predictive marker for chemosensitivity and chemotherapy response. *Clin Cancer Res* 13, 6344-6350, doi:10.1158/1078-0432.CCR-06-2682 (2007).

31 Bertolotto, C. *et al.* A SUMOylation-defective MITF germline mutation predisposes to melanoma and renal carcinoma. *Nature* 480, 94-98, doi:10.1038/nature10539 (2011).

32 Kauffman, E. C. *et al.* Molecular genetics and cellular features of TFE3 and TFEB fusion kidney cancers. *Nat Rev Urol* 11, 465-475, doi:10.1038/nrurol.2014.162 (2014).

33 Davis, I. J. *et al.* Oncogenic MITF dysregulation in clear cell sarcoma: defining the MiT family of human cancers. *Cancer Cell* 9, 473-484, doi:10.1016/j.ccr.2006.04.021 (2006).

34 Kuiper, R. P. *et al.* Upregulation of the transcription factor TFEB in t(6;11)(p21;q13)-positive renal cell carcinomas due to promoter substitution. *Hum Mol Genet* 12, 1661-1669 (2003).

35 Inamura, K. *et al.* Diverse fusion patterns and heterogeneous clinicopathologic features of renal cell carcinoma with t(6;11) translocation. *Am J Surg Pathol* 36, 35-42, doi:10.1097/PAS.0b013e3182293ec3 (2012).

36 Marchand, B., Arsenault, D., Raymond-Fleury, A., Boisvert, F. M. & Boucher, M. J. Glycogen synthase kinase-3 (GSK3) inhibition induces prosurvival autophagic signals in human pancreatic cancer cells. *J Biol Chem* 290, 5592-5605, doi:10.1074/jbc.M114.616714 (2015).

37 Argani, P. *et al.* A novel CLTC-TFE3 gene fusion in pediatric renal adenocarcinoma with t(X;17)(p11.2;q23). *Oncogene* 22, 5374-5378, doi:10.1038/sj.onc.1206686 (2003).

38 Clark, J. *et al.* Fusion of splicing factor genes PSF and NonO (p54nrb) to the TFE3 gene in papillary renal cell carcinoma. *Oncogene* 15, 2233-2239, doi:10.1038/sj.onc.1201394 (1997).

39 Ladanyi, M. *et al.* The der(17)t(X;17)(p11;q25) of human alveolar soft part sarcoma fuses the TFE3 transcription factor gene to ASPL, a novel gene at 17q25. *Oncogene* 20, 48-57, doi:10.1038/sj.onc.1204074 (2001).

40 Sidhar, S. K. *et al.* The t(X;1)(p11.2;q21.2) translocation in papillary renal cell carcinoma fuses a novel gene PRCC to the TFE3 transcription factor gene. *Hum Mol Genet* 5, 1333-1338 (1996).

41 Cronin, J. C. *et al.* Frequent mutations in the MITF pathway in melanoma. *Pigment Cell Melanoma Res* 22, 435-444, doi:10.1111/j.1755-148X.2009.00578.x (2009).

42 Garraway, L. A. *et al.* Integrative genomic analyses identify MITF as a lineage survival oncogene amplified in malignant melanoma. *Nature* 436, 117-122, doi:10.1038/nature03664 (2005).

43 Mahajan, J. & Stark, P. Barriers to education of overseas doctors in paediatrics: a qualitative study in South Yorkshire. *Arch Dis Child* 92, 219-223, doi:10.1136/adc.2006.098939 (2007).

44 Perera, R. M. *et al.* Transcriptional control of autophagy-lysosome function drives pancreatic cancer metabolism. *Nature* 524, 361-365, doi:10.1038/nature14587 (2015).

45 Medendorp, K. *et al.* The renal cell carcinoma-associated oncogenic fusion protein PRCCTFE3 provokes p21 WAF1/CIP1-mediated cell cycle delay. *Exp Cell Res* 315, 2399-2409, doi:10.1016/j.yexcr.2009.04.022 (2009).

46 Muller-Hocker, J., Babaryka, G., Schmid, I. & Jung, A. Overexpression of cyclin D1, D3, and p21 in an infantile renal carcinoma with Xp11.2 TFE3-gene fusion. *Pathol Res Pract* 204, 589-597, doi:10.1016/j.prp.2008.01.010 (2008).

47 McGill, G. G. *et al.* Bcl2 regulation by the melanocyte master regulator Mitf modulates lineage survival and melanoma cell viability. *Cell* 109, 707-718 (2002).

48 Dynek, J. N. *et al.* Microphthalmia-associated transcription factor is a critical transcriptional regulator of melanoma inhibitor of apoptosis in melanomas. *Cancer Res* 68, 3124-3132, doi:10.1158/0008-5472.CAN-07-6622 (2008).

49 Clevers, H. & Nusse, R. Wnt/beta-catenin signaling and disease. *Cell* 149, 1192-1205, doi:10.1016/j.cell.2012.05.012 (2012).

50 Ploper, D. *et al.* MITF drives endolysosomal biogenesis and potentiates Wnt signaling in melanoma cells. *Proc Natl Acad Sci U S A* 112, E420-429, doi:10.1073/pnas.1424576112 (2015).

51 Calcagni, A. *et al.* Modelling TFE renal cell carcinoma in mice reveals a critical role of WNT signaling. *Elife* 5, doi:10.7554/eLife.17047 (2016).

52 Di Malta, C. *et al.* Transcriptional activation of RagD GTPase controls mTORC1 and promotes cancer growth. *Science* 356, 1188-1192, doi:10.1126/science.aag2553 (2017).

53 Pollard, T. D. & Borisy, G. G. Cellular motility driven by assembly and disassembly of actin filaments. *Cell* 112, 453-465 (2003).

54 Chhabra, E. S. & Higgs, H. N. The many faces of actin: matching assembly factors with cellular structures. *Nat Cell Biol* 9, 1110-1121, doi:10.1038/ncb1007-1110 (2007).

55 Gupton, S. L. & Gertler, F. B. Filopodia: the fingers that do the walking. *Sci STKE* 2007, re5, doi:10.1126/stke.4002007re5 (2007).

56 Faix, J. & Rottner, K. The making of filopodia. *Curr Opin Cell Biol* 18, 18-25, doi:10.1016/j.ceb.2005.11.002 (2006).

57 Sanders, T. A., Llagostera, E. & Barna, M. Specialized filopodia direct long-range transport of SHH during vertebrate tissue patterning. *Nature* 497, 628-632, doi:10.1038/nature12157 (2013).

58 Stanganello, E. *et al.* Filopodia-based Wnt transport during vertebrate tissue patterning. *Nat Commun* 6, 5846, doi:10.1038/ncomms6846 (2015).

59 Moller, J., Luhmann, T., Chabria, M., Hall, H. & Vogel, V. Macrophages lift off surface-bound bacteria using a filopodium-

lamellipodium hook-and-shovel mechanism. *Sci Rep* 3, 2884, doi:10.1038/srep02884 (2013).

60 Phng, L. K. *et al.* Formin-mediated actin polymerization at endothelial junctions is required for vessel lumen formation and stabilization. *Dev Cell* 32, 123-132, doi:10.1016/j.devcel.2014.11.017 (2015).

61 Vignjevic, D. *et al.* Fascin, a novel target of beta-catenin-TCF signaling, is expressed at the invasive front of human colon cancer. *Cancer Res* 67, 6844-6853, doi:10.1158/0008-5472.CAN-07-0929 (2007).

62 Vasioukhin, V., Bauer, C., Yin, M. & Fuchs, E. Directed actin polymerization is the driving force for epithelial cell-cell adhesion. *Cell* 100, 209-219 (2000).

63 Davis, J. R. *et al.* Inter-cellular forces orchestrate contact inhibition of locomotion. *Cell* 161, 361-373, doi:10.1016/j.cell.2015.02.015 (2015).

64 Arjonen, A. *et al.* Mutant p53-associated myosin-X upregulation promotes breast cancer invasion and metastasis. *J Clin Invest* 124, 1069-1082, doi:10.1172/JCI67280 (2014).

65 Albuschies, J. & Vogel, V. The role of filopodia in the recognition of nanotopographies. *Sci Rep* 3, 1658, doi:10.1038/srep01658 (2013).

66 Lee, D., Fong, K. P., King, M. R., Brass, L. F. & Hammer, D. A. Differential dynamics of platelet contact and spreading. *Biophys J* 102, 472-482, doi:10.1016/j.bpj.2011.10.056 (2012).

67 Gardel, M. L., Schneider, I. C., Aratyn-Schaus, Y. & Waterman, C. M. Mechanical integration of actin and adhesion dynamics in cell migration. *Annu Rev Cell Dev Biol* 26, 315-333, doi:10.1146/annurev.cellbio.011209.122036 (2010).

68 Ridley, A. J. Rho GTPases and actin dynamics in membrane protrusions and vesicle trafficking. *Trends Cell Biol* 16, 522-529, doi:10.1016/j.tcb.2006.08.006 (2006).

69 Nobes, C. D. & Hall, A. Rho, rac and cdc42 GTPases: regulators of actin structures, cell adhesion and motility. *Biochem Soc Trans* 23, 456-459 (1995).

70 Machesky, L. M. & Insall, R. H. Scar1 and the related Wiskott-Aldrich syndrome protein, WASP, regulate the actin cytoskeleton through the Arp2/3 complex. *Curr Biol* 8, 1347-1356 (1998).

71 Rohatgi, R. *et al.* The interaction between N-WASP and the Arp2/3 complex links Cdc42-dependent signals to actin assembly. *Cell* 97, 221-231 (1999).

72 Stradal, T. E. & Scita, G. Protein complexes regulating Arp2/3-mediated actin assembly. *Curr Opin Cell Biol* 18, 4-10, doi:10.1016/j.ceb.2005.12.003 (2006).

73 Scita, G., Confalonieri, S., Lappalainen, P. & Suetsugu, S. IRSp53: crossing the road of membrane and actin dynamics in the formation of membrane protrusions. *Trends Cell Biol* 18, 52-60, doi:10.1016/j.tcb.2007.12.002 (2008).

74 Krugmann, S. *et al.* Cdc42 induces filopodia by promoting the formation of an IRSp53:Mena complex. *Curr Biol* 11, 1645-1655 (2001).

75 Miki, H. & Takenawa, T. WAVE2 serves a functional partner of IRSp53 by regulating its interaction with Rac. *Biochem Biophys Res Commun* 293, 93-99, doi:10.1016/S0006-291X(02)00218-8 (2002).

76 Disanza, A. *et al.* Regulation of cell shape by Cdc42 is mediated by the synergic actin-bundling activity of the Eps8-IRSp53 complex. *Nat Cell Biol* 8, 1337-1347, doi:10.1038/ncb1502 (2006).

77 Vaggi, F. *et al.* The Eps8/IRSp53/VASP network differentially controls actin capping and bundling in filopodia formation. *PLoS Comput Biol* 7, e1002088, doi:10.1371/journal.pcbi.1002088 (2011).

78 Mattila, P. K. *et al.* Missing-in-metastasis and IRSp53 deform PI(4,5)P2-rich membranes by an inverse BAR domain-like mechanism. *J Cell Biol* 176, 953-964, doi:10.1083/jcb.200609176 (2007).

79 Yamagishi, A., Masuda, M., Ohki, T., Onishi, H. & Mochizuki, N. A novel actin bundling/filopodium-forming domain conserved in insulin receptor tyrosine kinase substrate p53 and missing in metastasis protein. *J Biol Chem* 279, 14929-14936, doi:10.1074/jbc.M309408200 (2004).

80 Barzik, M. *et al.* Ena/VASP proteins enhance actin polymerization in the presence of barbed end capping proteins. *J*

Biol Chem 280, 28653-28662, doi:10.1074/jbc.M503957200 (2005).

81 Pasic, L., Kotova, T. & Schafer, D. A. Ena/VASP proteins capture actin filament barbed ends. *J Biol Chem* 283, 9814-9819, doi:10.1074/jbc.M710475200 (2008).

82 Ferron, F., Rebowski, G., Lee, S. H. & Dominguez, R. Structural basis for the recruitment of profilin-actin complexes during filament elongation by Ena/VASP. *EMBO J* 26, 4597-4606, doi:10.1038/sj.emboj.7601874 (2007).

83 Reinhard, M. *et al.* The 46/50 kDa phosphoprotein VASP purified from human platelets is a novel protein associated with actin filaments and focal contacts. *EMBO J* 11, 2063-2070 (1992).

84 Lanier, L. M. *et al.* Mena is required for neurulation and commissure formation. *Neuron* 22, 313-325 (1999).

85 Tokuo, H., Mabuchi, K. & Ikebe, M. The motor activity of myosin-X promotes actin fiber convergence at the cell periphery to initiate filopodia formation. *J Cell Biol* 179, 229-238, doi:10.1083/jcb.200703178 (2007).

86 DeRosier, D. J. & Edds, K. T. Evidence for fascin cross-links between the actin filaments in coelomocyte filopodia. *Exp Cell Res* 126, 490-494 (1980).

87 Mattila, P. K. & Lappalainen, P. Filopodia: molecular architecture and cellular functions. *Nat Rev Mol Cell Biol* 9, 446-454, doi:10.1038/nrm2406 (2008).

88 Ridley, A. J. *et al.* Cell migration: integrating signals from front to back. *Science* 302, 1704-1709, doi:10.1126/science.1092053 (2003).

89 Abercrombie, M., Heaysman, J. E. & Pegrum, S. M. The locomotion of fibroblasts in culture. II. "RRuffling". *Exp Cell Res* 60, 437-444 (1970).

90 Ponti, A., Machacek, M., Gupton, S. L., Waterman-Storer, C. M. & Danuser, G. Two distinct actin networks drive the protrusion of migrating cells. *Science* 305, 1782-1786, doi:10.1126/science.1100533 (2004).

91 Chen, W. T. Proteolytic activity of specialized surface protrusions formed at rosette contact sites of transformed cells. *J Exp Zool* 251, 167-185, doi:10.1002/jez.1402510206 (1989).

92 Buccione, R., Caldieri, G. & Ayala, I. Invadopodia: specialized tumor cell structures for the focal degradation of the extracellular matrix. *Cancer Metastasis Rev* 28, 137-149, doi:10.1007/s10555-008-9176-1 (2009).

93 Schoumacher, M., Goldman, R. D., Louvard, D. & Vignjevic, D. M. Actin, microtubules, and vimentin intermediate filaments cooperate for elongation of invadopodia. *J Cell Biol* 189, 541-556, doi:10.1083/jcb.200909113 (2010).

94 Friedl, P. & Gilmour, D. Collective cell migration in morphogenesis, regeneration and cancer. *Nat Rev Mol Cell Biol* 10, 445-457, doi:10.1038/nrm2720 (2009).

95 Wolf, K. & Friedl, P. Mapping proteolytic cancer cell-extracellular matrix interfaces. *Clin Exp Metastasis* 26, 289-298, doi:10.1007/s10585-008-9190-2 (2009).

96 Charras, G. & Paluch, E. Blebs lead the way: how to migrate without lamellipodia. *Nat Rev Mol Cell Biol* 9, 730-736, doi:10.1038/nrm2453 (2008).

97 Fackler, O. T. & Grosse, R. Cell motility through plasma membrane blebbing. *J Cell Biol* 181, 879-884, doi:10.1083/jcb.200802081 (2008).

98 Bovellan, M., Fritzsche, M., Stevens, C. & Charras, G. Death-associated protein kinase (DAPK) and signal transduction: blebbing in programmed cell death. *FEBS J* 277, 58-65, doi:10.1111/j.1742-4658.2009.07412.x (2010).

99 Kardash, E. *et al.* A role for Rho GTPases and cell-cell adhesion in single-cell motility in vivo. *Nat Cell Biol* 12, 47-53; sup pp 41-11, doi:10.1038/ncb2003 (2010).

100 Diz-Munoz, A. *et al.* Control of directed cell migration in vivo by membrane-to-cortex attachment. *PLoS Biol* 8, e1000544, doi:10.1371/journal.pbio.1000544 (2010).

101 Derivery, E. *et al.* Free Brick1 is a trimeric precursor in the assembly of a functional wave complex. *PLoS One* 3, e2462, doi:10.1371/journal.pone.0002462 (2008).

102 Petrie, R. J. & Yamada, K. M. At the leading edge of three-dimensional cell migration. *J Cell Sci* 125, 5917-5926, doi:10.1242/jcs.093732 (2012).

103 Shibue, T., Brooks, M. W. & Weinberg, R. A. An integrin-linked machinery of cytoskeletal regulation that enables experimental tumor initiation and metastatic colonization. *Cancer Cell* 24, 481-498, doi:10.1016/j.ccr.2013.08.012 (2013).

104 Fierro-Gonzalez, J. C., White, M. D., Silva, J. C. & Plachta, N. Cadherin-dependent filopodia control preimplantation embryo compaction. *Nat Cell Biol* 15, 1424-1433, doi:10.1038/ncb2875 (2013).

105 Machesky, L. M. & Li, A. Fascin: Invasive filopodia promoting metastasis. *Commun Integr Biol* 3, 263-270 (2010).

106 Li, A. *et al.* The actin-bundling protein fascin stabilizes actin in invadopodia and potentiates protrusive invasion. *Curr Biol* 20, 339-345, doi:10.1016/j.cub.2009.12.035 (2010).

107 Cao, R. *et al.* Elevated expression of myosin X in tumours contributes to breast cancer aggressiveness and metastasis. *Br J Cancer* 111, 539-550, doi:10.1038/bjc.2014.298 (2014).

108 Berg, J. S. & Cheney, R. E. Myosin-X is an unconventional myosin that undergoes intrafilopodial motility. *Nat Cell Biol* 4, 246-250, doi:10.1038/ncb762 (2002).

109 Yap, L. F. *et al.* Upregulation of Eps8 in oral squamous cell carcinoma promotes cell migration and invasion through integrin-dependent Rac1 activation. *Oncogene* 28, 2524-2534, doi:10.1038/onc.2009.105 (2009).

110 Zhu, X. L. *et al.* FMNL2 is a positive regulator of cell motility and metastasis in colorectal carcinoma. *J Pathol* 224, 377-388, doi:10.1002/path.2871 (2011).

111 Kitzing, T. M., Wang, Y., Pertz, O., Copeland, J. W. & Grosse, R. Formin-like 2 drives amoeboid invasive cell motility downstream of RhoC. *Oncogene* 29, 2441-2448, doi:10.1038/onc.2009.515 (2010).

112 Gurzu, S., Ciortea, D., Ember, I. & Jung, I. The possible role of Mena protein and its splicing-derived variants in embryogenesis, carcinogenesis, and tumor invasion: a systematic review of the literature. *Biomed Res Int* 2013, 365192, doi:10.1155/2013/365192 (2013).

113 Bohil, A. B., Robertson, B. W. & Cheney, R. E. Myosin-X is a molecular motor that functions in filopodia formation. *Proc Natl Acad Sci U S A* 103, 12411-12416, doi:10.1073/pnas.0602443103 (2006).

114 Albini, A. *et al.* A rapid in vitro assay for quantitating the invasive potential of tumor cells. *Cancer Res* 47, 3239-3245 (1987).

115 Repesh, L. A. A new in vitro assay for quantitating tumor cell invasion. *Invasion Metastasis* 9, 192-208 (1989).

116 Funato, Y. *et al.* IRSp53/Eps8 complex is important for positive regulation of Rac and cancer cell motility/invasiveness. *Cancer Res* 64, 5237-5244, doi:10.1158/0008-5472.CAN-04-0327 (2004).